

**A THIN FILM POLYMER SYSTEM FOR THE PATTERNING OF AMINES
THROUGH THERMOCHEMICAL NANOLITHOGRAPHY**

A Thesis
Presented to
The Academic Faculty

By

William David Underwood II

In Partial Fulfillment
Of the Requirements for the Degree
Master of Science in Chemistry

Georgia Institute of Technology

August, 2009

A THIN FILM POLYMER SYSTEM FOR THE PATTERNING OF AMINES
THROUGH THERMOCHEMICAL NANOLITHOGRAPHY

Approved by:

Dr. Seth Marder
School of Chemistry and Biochemistry
Georgia Institute of Technology

Dr. Elisa Riedo
School of Physics
Georgia Institute of Technology

Dr. Jennifer Curtis
School of Physics
Georgia Institute of Technology

Date Approved: August 20, 2009

ACKNOWLEDGMENTS

I would like to acknowledge my research advisor, Seth Marder, for supporting this research both intellectually and financially. I would also like to thank the entire Marder group in general and Takashi Okada, Jonas Jarvholm, Mariacristina Rumi, and Anthony Giordano specifically for all of their assistance. I would like to thank my collaborators, Elisa Riedo, Debin Wang, Jennifer Curtis, and Vamsi Kodali for all of their work on furthering this research. I would like to thank my parents for their advice and support on transitioning into my graduate studies. Finally I would like to thank my wife, Carol for her willingness to live like a pauper for three years and move across half the country so I could pursue my interests.

TABLE OF CONTENTS

ACKNOWLEDGMENTS.....	iii
LIST OF TABLES.....	vi
LIST OF FIGURES.....	vii
GLOSSARY (SYMBOLS AND ABBREVIATIONS)	ix
SUMMARY.....	xi
INTRODUCTION OF NANOLITHOGRAPHY TECHNIQUES AND APPLICATIONS	1
1.1 Photolithography: The Industrial Standard.....	1
1.2 Scanning Probe Lithography: Nanoscale Techniques.....	2
1.3 Nanolithography Applications: Biological Arrays.....	8
1.4 Goals and objectives.....	10
CHAPTER 2: DEVELOPMENT OF A THERMALLY-PROTECTED AMINE POLYMER	11
2.1 Introduction.....	11
2.2 Synthesis.....	12
2.3 Characterization.....	14
2.4 Pyrolysis.....	19
2.5 Summary.....	29
CHAPTER 3: DEVELOPMENT AND CHARACTERIZATION OF POLYMER FILMS	31
3.1 Introduction.....	31
3.2 Preparation of Polymer Films.....	31
3.3 Characterization of Polymer Films.....	35
3.4 Summary.....	42
CHAPTER 4: PATTERNING OF PRIMARY AMINES AND PPV.....	43
4.1 Reactive Amine Patterns.....	43
4.1.1 Introduction.....	43
4.1.2 Bulk Test of Fluorescent procedure.....	43
4.1.3 Micropatterns.....	45
4.2 Patterns of Polyphenylenevinylene (PPV).....	47
4.2.1 Background.....	47
4.2.2 Procedures.....	48
CHAPTER 5: CONCLUDING REMARKS	50
APPENDIX A: EXPERIMENTAL METHODS.....	52

REFERENCES.....

60

LIST OF TABLES

Table 1	Typical thicknesses of polymer films based on concentration (mg / ml) and spin speed (RPM)	32
Table 2	Average fluorescence (in arbitrary units) of polymer films	45
Table 3	Observations of slides coated under different conditions	48

LIST OF FIGURES

Figure 1	A graphical depiction of the process of TCNL; thermal conversion of the ester to the carboxylic acid	6
Figure 2	Possible functionality conversions that could be potentially used for TCNL	7
Figure 3	Cinnamate and carbamate monomers and the copolymer and expected decomposition products	11
Figure 4	Crosslinking mechanism of the cinnamate monomer (1).	12
Figure 5	Synthetic route to the carbamate monomer (2) and the two conformers of THP. Synthetic route to the cinnamate monomer (1)	13
Figure 6	Synthesis of the cinnamate – carbamate copolymer (3)	14
Figure 7	¹ H NMR spectra of the carbamate monomer and polymer and peak assignments	15
Figure 8	FT-IR spectrum of 3 (KBr disk)	16
Figure 9	TGA (5 °C / min) and isothermal TGA (held 30 min. at each of 170 °C and 220 °C) of carbamate copolymer 3	18
Figure 10	The most probable decomposition pathways of the THP-carbamate moiety	19
Figure 11	Structure and pyrolysis of 10 , ¹ H NMR spectrum of 10 in nitrobenzene- <i>d</i> ₅ both before and after refluxing, ¹ H NMR of DHP	21
Figure 12	Synthetic pathway to tetrahydropyran-2-yl dodecylcarbamate	22
Figure 13	TGA of 14 and Isothermal TGA of 14	24
Figure 14	Dodecylamine and Dodecylisocyanate before and after refluxing in nitrobenzene	25
Figure 15	Comparison of DHP to 14 pyrolyzed in nitrobenzene- <i>d</i> ₅ . ¹ H NMR spectra of pyrolyzed 14 , the original material, and the most likely products	28

Figure 16	Reaction scheme for the synthesis of 17 .	33
Figure 17	Photocrosslinking of the cinnamate moiety in the polymer films. IR of spectra of a carbamate film before and after irradiation	36
Figure 18	UV-Vis and FT-IR spectra of polymer before and after exposing to 354 nm and / or 300 nm radiation	38
Figure 19	Pyrolysis of the carbamate moiety	40
Figure 20	IR of spectra of carbamate films heated to different temperatures	41
Figure 21	Scheme for the preparation of bulk fluorescence samples	44
Figure 22	10 μm squares patterned by TCNL and conjugated fluorescent probes with friction measurements	46
Figure 23	Thermal conversion of 19 into PPV (20)	47
Figure 24	The word PPV written through the thermal conversion of poly 19 onto PPV	49

LIST OF ABBREVIATIONS

AFM	atomic force microscopy
AIBN	azobisisobutyronitrile
SPM	Scanning Probe Microscopy
b.p.	boiling point
cAFM	conducting atomic force microscopy
DHP	dihydropyran
DMSO	dimethylsulfoxide
DPN	dip pen nanolithography
ECM	extracellular matrix
FITC	fluorescein isothiocyanate
FT-IR	Fourier transform infrared
NMR	nuclear magnetic resonance
PEG	poly(ethylene glycol)
PPV	polyphenylene vinylene
RPM	revolutions per minute
TCNL	thermochemical nanolithography
T_d	temperature of decomposition
tDPN	thermal DPN
T_g	glass transition temperature
TGA	thermal gravimetric analysis
THP	tetrahydropyran
μ CP	microcontact printing

UV

ultraviolet

SUMMARY

A system for the patterning of amines through the thermal decomposition of a thin polymer film was proposed. The polymer was synthesized and films were produced by spin coating. The pyrolysis of both the polymer and the films was studied. The physical properties of the film, such as T_g , were controlled through crosslinking of the polymer and the crosslinking conditions were optimized. Analyses of the reactions that occur on the film as a result of thermal decomposition were studied. These studies seem to indicate that the thin film system studied is viable option toward the patterning of amines. The ability to bind material to the polymer films after deprotection was demonstrated using fluorescent protein and fluorescein isothiocyanate. Micron scale patterns of these fluorescent molecules were created and imaged, successfully demonstrating the viability of the system for patterning. Patterns of polyphenylene vinylene were produced through the thermal decomposition of a tetrahydrothiophenium chloride salt precursor. Images of the patterns were obtained.

INTRODUCTION OF NANOLITHOGRAPHY TECHNIQUES AND APPLICATIONS

1.1 Photolithography: The Industrial Standard

Modern technology has inarguably been greatly affected by the advancements in one particular field, computing. The use of silicon-chip based technology has become so universal in developed nations that it is nearly inconceivable for society to operate without it. The rapid development of silicon-based chips was made possible by the ability to continually miniaturize the size of transistors used, allowing more to be made within the same space.¹ These advances have been driven by the improvements of the manufacturing technique used to pattern the silicon chip: photolithography. The photolithographic process generally involves the exposure of a resist to a light source and the washing away of either the exposed or unexposed portion of the resist. If the resist becomes insoluble, then the patterned area remains after washing. These types of resist are called negative resists. If the resist becomes soluble, then only the patterned area is washed away. These resists are called positive resists. After removal of the soluble portion of the resist, the entire surface is exposed to an etching agent and any portion of the silicon surface not protected by resist is etched, forming the pattern. The theoretical limits of this methodology are dependent upon the wavelength of light used, while the practical limits also depend upon the cost and availability of resists, lenses, and photomasks useable at that wavelength.¹ The wavelengths available for industrial use have been gradually reduced from 436 nm in the 1960s to the current standards of 195 and 157 nm radiation, improving the available resolution.¹ As the wavelength decreases, however, the costs associated with the manufacturing process increase. The physical

limit for the line width using these wavelengths is thought to be around 45 nm and is rapidly being approached by modern technology.¹ As it becomes increasingly difficult to increase the resolution of photolithography in an economical fashion, alternative methods of lithography are in demand for small-scale fabrication.

Other non-silicon based applications of photolithography also exist, a prime example being the patterning of DNA arrays.² These applications generally require the extreme limits in resolution available, causing experiments to be expensive and time consuming.² Also, for most biological applications, mild conditions are a necessity in order to avoid denaturing the proteins being patterned, which limits some of the possible alternatives to photolithography.

1.2 Scanning Probe Lithography: Nanoscale Techniques

An ideal nanolithographic technique is one that is capable of producing precise (nm resolution) and rapid (cm/s) changes in the chemical and/or physical properties of a material that can be adapted to a variety of substrates under conditions mild enough to be compatible with sensitive applications, such as those involving proteins.³ Preferably, a method of parallelization would also be available, allowing the rapid production of large scale patterns.³ No methodology currently in use can simultaneously achieve each of these objectives. As such, the choice of the lithographic methodology, and its associated limitations and strengths, is quite important when considering which methodology to use for any given application.

Scanning probe microscopy (SPM) has, since its inception in 1981, become a widely popular technique for the determination of the properties of surfaces on the

nanometer level.^{3, 4} Due to the capability of SPM to interact with surfaces on such a small scale it has been used as the basis for several lithographic techniques in the hopes that they may provide an economically feasible replacement for current lithographic methods, such as photolithography, that are swiftly approaching the physical limits of their resolution.³

One promising family of nanolithographic techniques currently being developed has its basis in atomic force microscopy (AFM). These techniques create various patterns by using an AFM tip to either remove material from or add material to a substrate, or to directly modify the surface either chemically or physically.³ The removal of material can be achieved through simple mechanical scratching of the surface with the AFM tip by applying force, etching the surface like a chisel.³ The resulting mechanical strain causes the tip to wear quickly and the etching depth obtainable is limited by the length of the tip. An alternate technique that takes advantage of the second vibrational mode of the AFM cantilever has recently been reported for the patterning of proteins.⁵ Typically, tapping mode AFM operates in the first vibrational mode, where the vibrational wavelength is twice the length of the cantilever. This maximizes the height change at the tip and allows larger feature sizes to be observed. Adjusting the vibrational amplitude can force the cantilever into the second vibrational mode, where the wavelength is identical to the cantilever length, causing the tip to oscillate rapidly without significant vertical displacement.⁵ Bringing the vibrating tip into contact with an adhered monolayer of protein on the surface results in several of the proteins being removed from the surface. The displaced proteins are then washed away and new protein added, creating the desired pattern.⁵ Repeating this procedure allows for the patterning of multiple proteins with

feature sizes as small as 50 nm on the same sample. However, the requirement that a monolayer of proteins already be present limits the compatibility of some substrates and excludes certain experiments that require a low density of patterned proteins.

The two techniques described above involve the removal of material through physical contact. Material can also be removed by degradation through the application of either heat or electricity. A conducting AFM (cAFM) tip can remove material in a nearly identical manner to e-beam lithography, only using less rigorous conditions, improved resolution, and less energy.³

The second mechanism for nanopatterning with an AFM is through the addition of material to a substrate. One of the more powerful and versatile nanolithographic techniques currently developed, dip pen nanolithography (DPN), creates patterns through material addition. DPN, first reported in 1998, was first used to create patterns of alkyl thiols on gold surfaces.⁶ This technique involves several steps. First, an AFM tip is coated with a molecular “ink,” such as octylthiol. The second step begins with the tip being brought into contact with the surface. Upon approach to the surface a water meniscus forms between the tip and the surface. The “ink” molecule then diffuses across this meniscus onto the substrate. Finally, the AFM tip is dragged across the surface, creating a pattern of adhered “ink” molecules until the tip is retracted.^{3,6-8} DPN has been used to pattern a wide variety of materials including proteins, cells, polymers, small organic molecules, sols, and even metals.^{6,7} Erasure capabilities for DPN have recently been developed, allowing for patterning mistakes to be corrected.⁸ This is achieved through the application of a voltage bias between the tip and the substrate, causing the patterned material to return to the tip, allowing for the removal of undesired patterning.

Although a versatile technique, DPN has several limitations. First is the writing speed, which is limited by the rate of diffusion of the molecular ink. This weakness has been somewhat mitigated with the development of thermal DPN (tDPN). tDPN heats the “ink”-coated AFM tip during normal DPN operation. This allows normally solid and insoluble materials to be patterned and the temperature of operation can be used to control the rate of diffusion achieved.⁷ A second weakness of DPN is its sensitivity to ambient conditions such as humidity and temperature. A higher humidity causes the water meniscus between the tip and substrate to be larger, causing a subsequent increase in pattern size.^{3, 9} Finally, as DPN requires the “ink” to adhere strongly enough to the substrate that it remains behind as the tip drags the water meniscus away. This can often limit the number of substrates compatible with any given “ink.”³

The third mechanism for nanopatterning, direct physical or chemical modification of substrates, has been achieved through a process known as thermomechanical nanolithography. In this process, an AFM tip is brought into contact with a polymer film and pulses of current are run through the cantilever creating heat through resistance. The heat travels through the AFM tip, melting the substrate in the region near the tip. The force applied to the tip drives it into the melted substrate, creating a depression.^{3, 10-12} This process is thought to have great potential as a writing mechanism in data storage applications.^{3, 10-12} A similar technique developed more recently, called *thermochemical* nanolithography (TCNL), also uses a resistively heated AFM tip. The key difference in these techniques is that TCNL uses the tip to cause chemical changes through pyrolysis of the surface (Figure 1A) rather than physical changes through mechanical depression or melting.^{9, 13} This technique was first demonstrated through the thermal conversion of a

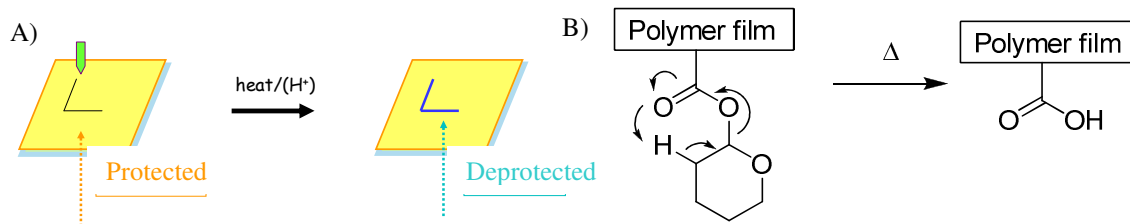


Figure 1: A) A graphical depiction of the process of TCNL; B) thermal conversion of the ester to the carboxylic acid.

tetrahydropyranyl ester groups attached to a poly(methylmethacrylate) backbone into a carboxylic acids (Figure 1B), achieving a spatial resolution as small as 12 nm.⁹ It was also found that further heating of the surface converts the carboxylic acid into an anhydride.¹³

The ability to convert a hydrophobic surface (initial ester surface) to a hydrophilic pattern (deprotected carboxylic acids) and then back to hydrophobic (anhydrides) holds promise as a technique for studying nanofluidics.^{9, 13} One interesting aspect of this technique is that careful selection of the temperature of decomposition (T_d) of the protected functionality and the glass transition temperature (T_g) of the film allows for both physical and chemical changes to be made either separately or simultaneously.⁹ The greatest strength of TCNL is that the speed is limited by thermal, not molecular, diffusion. Typical rates of thermal diffusion place the potential writing speeds at three orders of magnitude greater than those of DPN.⁹ While the ability to pattern carboxylic acids and anhydrides could be useful for various applications like nanofluidics¹³ or the bending of carbon nanotubes,^{7, 14} in order for TCNL to be a competitive technique it must be expanded to other functionalities.

Heated AFM tips have been used to achieve chemical changes before,^{11, 15} but none has created a reactive pattern that was then chemically modified. Previously, the heated AFM tip has been used to either crosslink a resist, in an analogous fashion to current photolithography except without the use of a mask,¹⁵ or it has been used to drive a reverse Diels-Alder reaction, breaking down a polymer for use in data storage.¹¹ Neither of these studies used the heated AFM tip to create a chemically active surface for post modification.

Several promising functionalities that form chemically reactive moieties upon thermal decomposition can be found in literature. Examples include the formation of amines from the pyrolysis of carbamates,¹⁶ thiols from xanthates,¹⁷ and alcohols from carbonates¹⁸ (Figure 2). There are numerous known conjugation methods available for each of these functional groups that have been studied extensively by biologists.¹⁹ The patterning of these functional groups could greatly expand the potential applications of techniques to be utilized.

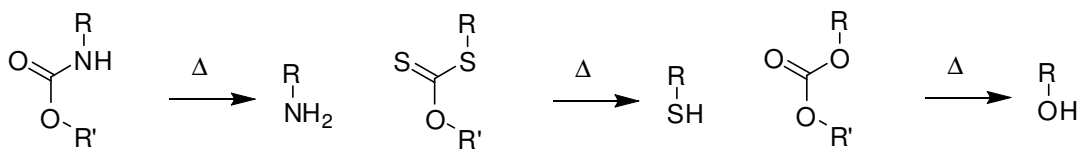


Figure 2: Possible functionality conversions that could be potentially used for TCNL. TCNL beyond those available with carboxylic acids and allow these conjugation

1.3 Nanolithography Applications: Biological Arrays

A potential application of nanolithography is the formation of arrays of biological molecules on surfaces. Such arrays can be used for a variety of applications including cell adhesion,^{2, 20-22} microfabrication,^{2, 23} and combinatorial studies.² Many cells, including most mammalian cells, require a surface of proteins to adhere to for proper functionality and the properties of that surface often greatly influence the cell's behavior.^{20, 21} The various proteins and other molecules to which cells adhere in nature are called the extracellular matrix (ECM). The ECM not only serves to provide a mechanical scaffold for the cells, but also provides communication pathways and directs cell function.²⁰ The study of the ECM requires that the natural system be mimicked in a laboratory setting, typically through the adhesion of proteins to a substrate through covalent binding² or adsorption to hydrophobic surfaces.^{2, 20, 21} The choice of proteins used depends on the cell or cell process being studied. The patterning of proteins onto surfaces has been found to be quite useful for studying the effects that changes to the ECM has on cells, and allows cells to be immobilized in known regions.^{2, 21}

Immobilization of cells at specific locations allows individual cells to be studied and then located and analyzed again after an experiment has been performed.²⁰ Also, the patterning of individual proteins at specific locations allows more rigorous studies of the effects that different properties of the ECM, such as protein spacing, have on the cell. So far, DPN has been successfully used to pattern proteins onto surfaces but has been unable to achieve single protein resolution, though it has successfully patterned single viruses.⁷

Controlling the adhesion of proteins requires the creation of patterned regions where the protein adhesion is energetically unfavorable and regions where protein

adhesion is energetically favorable. This is complicated by the tendency of proteins to adhere to most surfaces. The simplest solution involves creating a negative pattern using a material that resists protein and, preferably, cell adhesion. One of the few chemicals that can successfully resist both protein and cell adhesion without destroying either is poly(ethylene glycol) (PEG).^{2, 20} Patterns of PEG are commonly created using a process known as microcontact printing (μ CP).² This technique involves creating a “stamp” with the desired pattern and then coating it with the substrate. The stamp is then brought into contact with the surface, transferring the material from any raised portions of the stamp to the surface through adhesion forces.² The greatest strength of μ CP is that it is simple to use once a stamp has been made. Production of patterns with line widths as small as 1 μ m are routine and line widths as small as 40 nm can be made, though with more difficulty.² Each stamp, however, can only make a single pattern, requiring researchers to obtain a new stamp for each desired change in the pattern properties, such as protein spacing. This problem is not an issue with nanolithographic techniques such as TCNL and DPN.

Finally, any lithographic technique requires a method for parallelization, allowing for the rapid production of a large number of patterns simultaneously, if it is to be useful for the industrial production of nanoscale devices. TCNL could potentially gain this parallelization through coupling with a device currently being developed by IBM. This device, known as the Millipede, consists of an array of AFM tips with independent control of both the height and temperature of each tip.^{10, 12} Use of this tip array (32 \times 32 tips) would impart massive parallelization to TCNL, a useful trait if it is to become an industrially viable lithographic technique in the future.

1.4 Goals and Objectives

In this thesis a system designed to produce reactive amine patterns through TCNL is proposed and discussed. The proposed system involves the creation of thin films of a thermally-protected amine polymer that can be heated to over 200 °C without physical deformation. The polymer is designed, synthesized, and characterized as described in Chapter II. The thermal decompositions of this polymer are also explored. In chapter III, the creation and characterization of thin films using the polymer from Chapter II are discussed. Steps are made towards the optimization of film processing and the chemical reactions involved in the proposed system are identified. Chapter IV demonstrates the capabilities of TCNL to pattern the films made in Chapter III. Chapter IV also discusses the use of TCNL to create patterns of a conductive polymer using films of commercially available materials.

CHAPTER II: DEVELOPMENT OF A THERMALLY-PROTECTED AMINE POLYMER

2.1 Introduction

Amine functional groups have been used by biologists for years as a means of conjugating proteins to a variety of small molecules and surfaces.^{19, 24} Patterned surfaces of primary amines have also been used to covalently bind fullerene molecules.²⁵ Thermal generation of primary amines is achievable through the pyrolysis of carbamates through known mechanisms, though alternative decomposition pathways exist.^{16, 26, 27} By performing TCNL on surfaces composed of carbamate containing polymer the chemical flexibility of amines should become accessible.

To this end, a carbamate-containing copolymer was synthesized from a mixture of methacrylate monomers, one possessing a cinnamate that had been reported previously²⁸

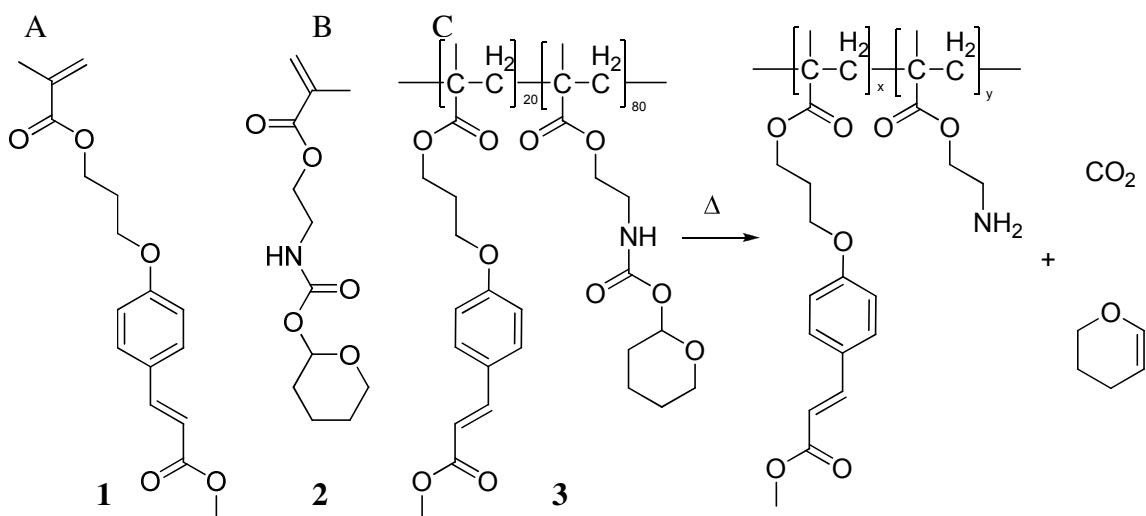


Figure 3: A) Cinnamate and B) carbamate monomers and the C) copolymer and expected decomposition products.

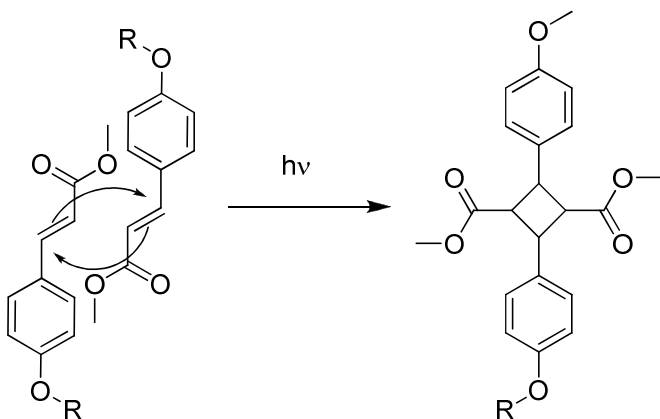


Figure 4: Crosslinking mechanism of the cinnamate monomer (1).

(1, Figure 3A) and the other a novel carbamate shown in Figure 3B (2). The protecting group chosen was tetrahydropyran (THP) as the resulting carbamate was expected to decompose at a relatively low temperature. A low T_d is advantageous as it allows TCNL to operate at lower temperatures, reducing the likelihood of undesired side reactions or decompositions. The cinnamate was incorporated into the copolymer in order to provide a mechanism to control the T_g of the polymer. The cinnamate group accomplishes this through the crosslinking reaction shown in Figure 4. As the purpose of this study was to understand the chemical changes brought about in the polymer system independent of any topological changes an increased T_g was necessary.

2.2 Synthesis

The carbamate monomer tetrahydropyran-2-yl N-(2-methacryloxyethyl)carbamate (2) was synthesized as shown in Figure 5A. The THP protecting group was used because it had been successfully incorporated as a low T_d protecting group for an ester polymer previously studied.^{9, 13} The monomer was synthesized by dissolving 2-isocyanatoethyl

methacrylate (**4**) in tetrahydropyran-2-ol (**5**), which was prepared by a reported procedure,²⁹ and adding one a catalytic amount of pyridine at room temperature. After the reaction was complete according to ¹H nuclear magnetic resonance (NMR) spectroscopy the product was purified by column chromatography. Analysis of the ¹H NMR spectrum suggests the presence of two different conformers most likely caused by the anomeric effect (Figure 5B). The anomeric effect is the preference for the axial conformer of tetrahydropyrans with an electronegative substituent in the 2 position.³⁰ The ratio of the major to the minor conformer, measured by the relative areas of the two peaks observed for the N-H peak and the hydrogen at the 2 position on the THP in the ¹H NMR, was approximately 4 to 1. The cinnamate monomer (**1**) was synthesized according to a literature procedure shown in Figure 5C.²⁸ This molecule was formed through a Williamson ether syntheses followed by a Steglich esterification.

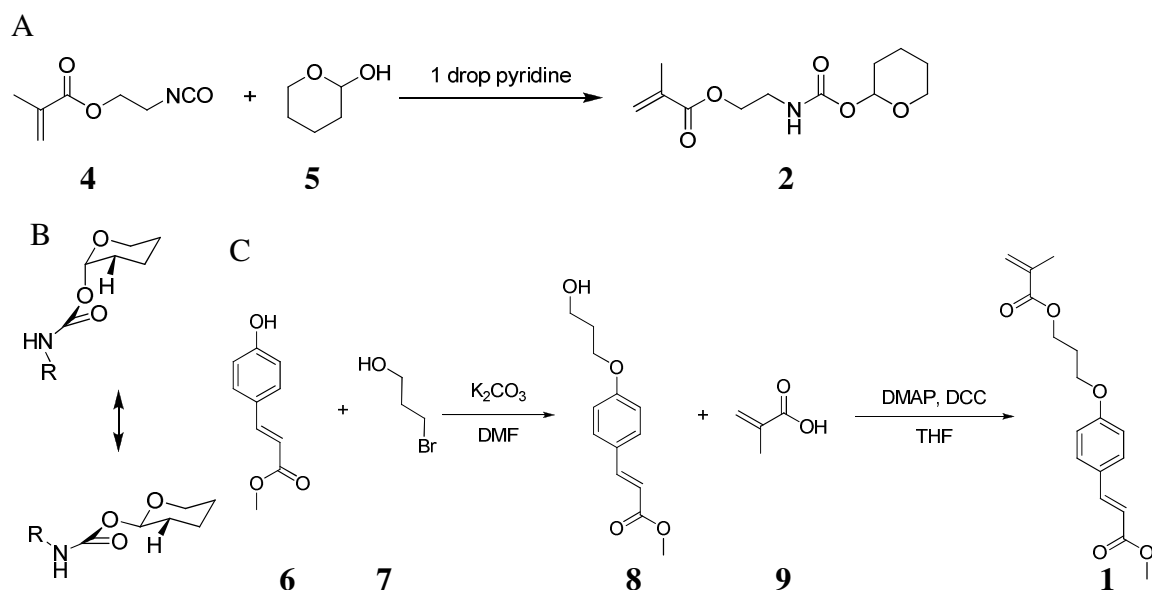


Figure 5: A) Synthetic route to the carbamate monomer (**2**) and B) the two conformers of THP. C) Synthetic route to the cinnamate monomer (**1**)

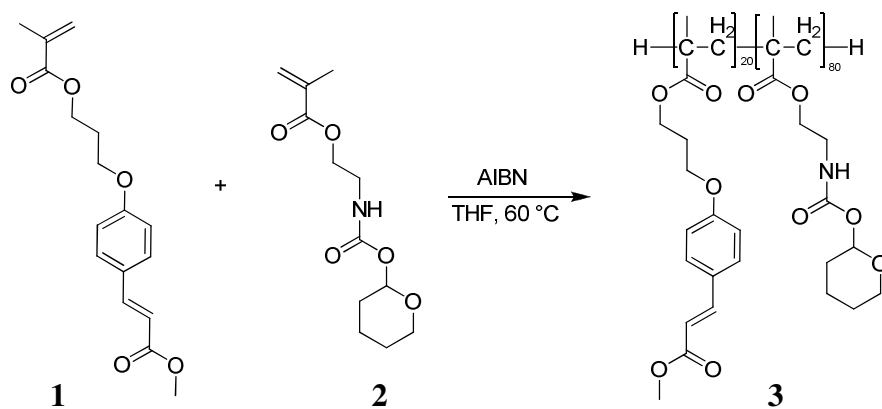


Figure 6: Synthesis of the cinnamate-carbamate copolymer (**3**).

Polymerization of the two synthesized monomers was carried out through a radical polymerization using azobisisobutyronitrile (AIBN, Figure 6). The ratio of monomer **1** to monomer **2** was set to 1 : 4 in order to provide for a good density of crosslinking while hopefully not greatly reducing the available density of amines upon deprotection. Analysis of the ^1H NMR, reported in Appendix A, suggests a lower relative amount of the carbamate monomer (**2**) than a perfect 1 to 4 cinnamate to carbamate ratio. Elemental analysis, on the other hand, suggests a slightly higher relative amount of monomer **2** than expected. However, the expected ratio was within the uncertainty of both of these measurements so a 1 to 4 cinnamate to carbamate ratio was assumed.

2.3 Characterization

The carbamate monomer (**2**) was first characterized by ^1H NMR spectroscopy as seen in Figure 7A. Peaks are assigned based on the chemical shift and integration values and are numbered in Figure 7A below. The amine hydrogen and the hydrogen on the

THP 2 position, labeled 5 and 6 in Figure 7A, were distinguished by adding a small aliquot of D₂O to the CDCl₃ solution used to obtain the NMR spectrum. The only change was the disappearance of the two peaks around 5.0 ppm and the appearance of a peak 4.7 ppm associated with water dissolved in the D₂O layer that formed. Figure 7B shows the ¹H NMR spectrum of the co-polymer **3**. The most notable change was that all the peaks were significantly broader than for the two monomers. This was expected as the polymer repeating units will each be in slightly different magnetic environments, causing slight changes in the chemical shifts that broaden the peaks. The aromatic peaks of the cinnamate appear at 7.6, 7.5, 6.9, and 6.3 ppm, denoted by the letters c, b, a, and d in

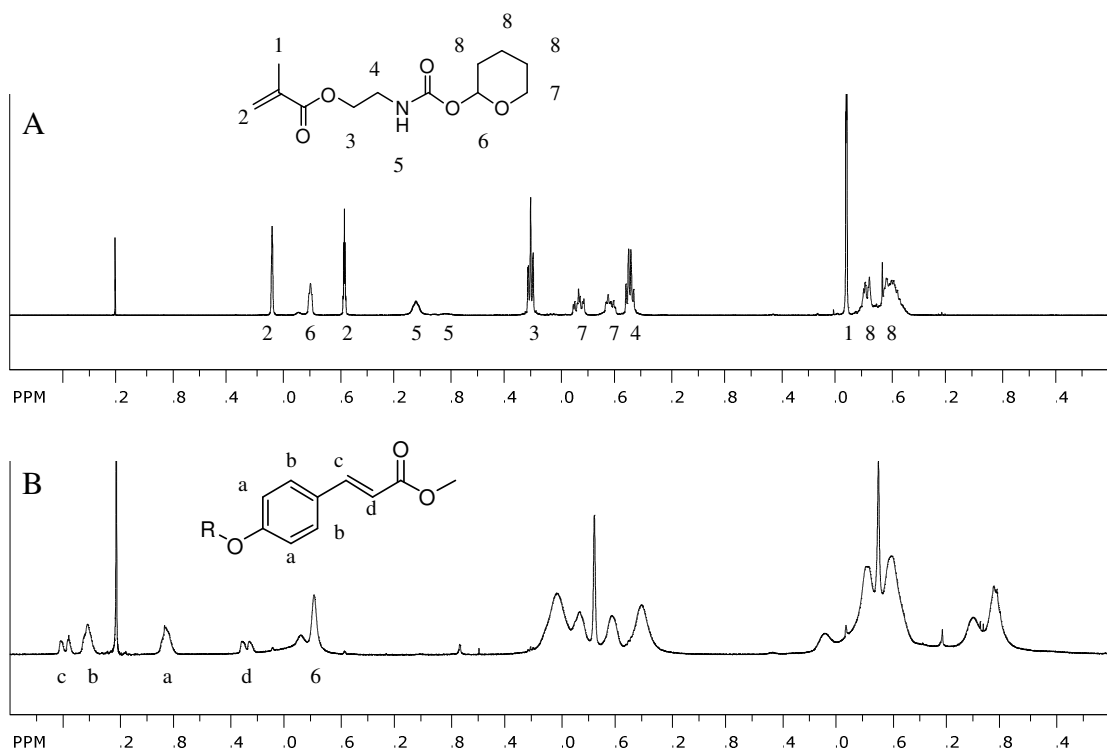


Figure 7: ¹H NMR spectra of the carbamate a) monomer and b) polymer and peak assignments.

Figure 7B respectively. The assignment of these peaks is based on their integration – a and b integrate for 2 H while c and d integrate for only 1 – and chemical shift. The chemical shift of c and b would be expected to be relatively deshielded due to conjugation with the ester carbonyl through the double bonds. The other noticeable difference is the disappearance of the peaks at 6.1 and 5.6 ppm. These peaks are associated with the double bond of the methacrylate group and were expected to be lost during polymerization. The resulting hydrogens, attached directly to the polymer backbone, are most likely responsible for the appearance of the peaks around 0.8 ppm. The observed ^1H NMR spectrum is consistent with the structure of **3**, as shown in Figure 6, and indicates that the synthesis was successful.

An FT-IR transmittance spectrum of polymer **3** is shown in Figure 8. The most easily identified features were the N-H stretching peak between $3300 - 3400\text{ cm}^{-1}$ and the

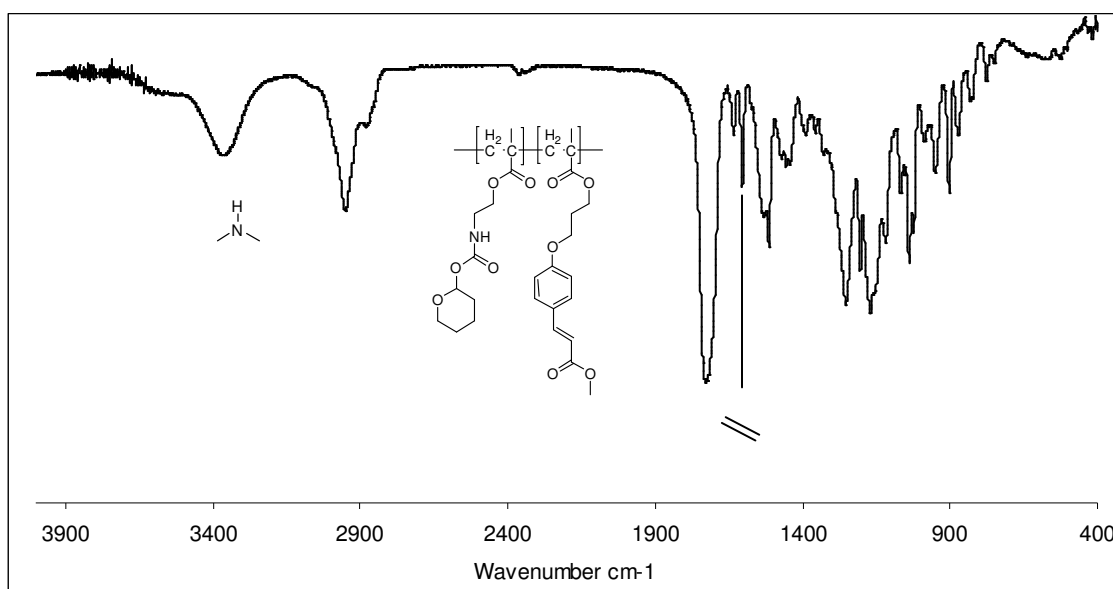


Figure 8: FT-IR spectrum of **3** (KBr disk).

carbonyl stretching mode at 1717 cm^{-1} . It is notable that there is only one carbonyl peak in Figure 8 even though there were several carbonyl groups in the polymer. This is most likely due to overlap of the carbonyl peaks, which would also explain why the peak is so broad. Another notable feature was a band assignable to the carbon-carbon double bond stretching mode from the cinnamate at about 1605 cm^{-1} . That this peak was distinguishable from the aromatic stretch (broad absorption at approximately 1510 cm^{-1}) made FT-IR studies of the crosslinking of the film discussed below possible. The other peaks in the IR are difficult to identify due to their breadth.

As TCNL depends upon the pyrolysis of the surface being patterned, a good understanding of the temperature of decomposition of polymer **3** was necessary. The first step to gain this understanding was to perform thermal gravimetric analysis (TGA) on the material (heating rate $5\text{ }^{\circ}\text{C}/\text{min}$, Figure 9A). The TGA trace possessed a step shape, with a plateau at about $170\text{ }^{\circ}\text{C}$ and a second flat region at about $220\text{ }^{\circ}\text{C}$. There are two likely causes for this feature in the TGA. First, the decomposition mechanism could be made up of an initial fast step followed by a slow step. Such a situation would resemble a second decomposition if the second step was slow enough that it took several minutes. Second, the different conformers of the THP group could have different T_d . The possibility that the pyrolysis stabilizes at the carbamic acid intermediate is unlikely as this would result in a mass loss of 25 %, not the observed 33 %. Also, the carbamic acid would most likely be less stable than the original carbamate precluding it from requiring a higher temperature of decomposition.

To determine which of these possibilities was responsible for the feature in the TGA, an isothermal TGA was obtained by holding the temperature constant for 30

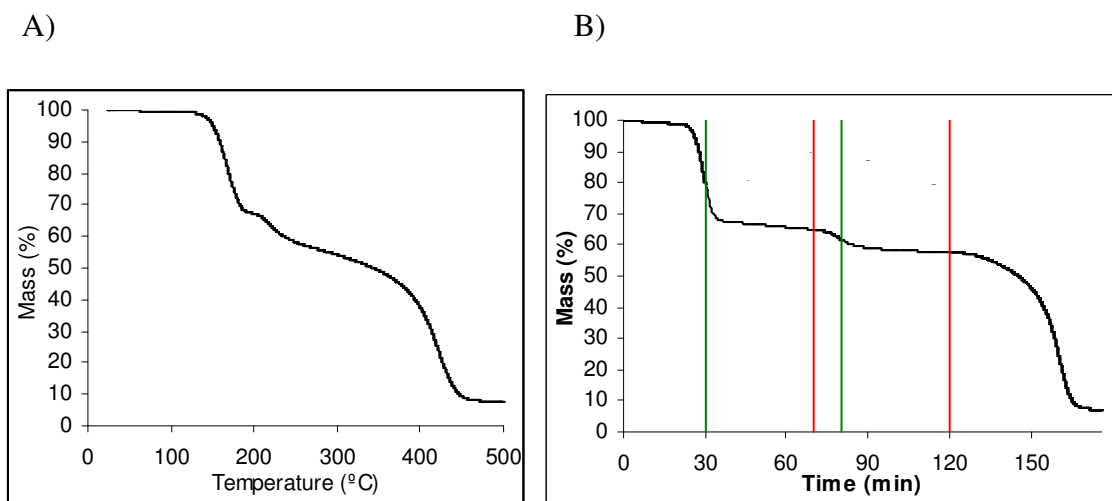


Figure 9: A) TGA (5 °C / min) and B) isothermal TGA (held 30 min. at each of 170 °C and 220 °C) of carbamate copolymer **3**. The green line represents the beginning and the red line represents the end of the isothermal portions.

minutes in the regions where the two features shown in Figure 9A were observed, 170 °C and 220 °C (Figure 9B). The isothermal TGA showed that the second mass loss step did not occur until after the material was further heated. If the observed feature had been the result of a rapid decomposition step followed by a slower one then a similar feature as in Figure 9A would have been observed during the time the temperature was held at 170 °C. Since the polymer did not experience any additional mass loss until the temperature was raised to 220 °C the feature was most likely caused by the presence of the different conformers, each with a different T_d , of the THP observed in the ^1H NMR. The ratio of the two mass loss steps was 33 to 8, or approximately 4 to 1, which was the same ratio observed in the carbamate monomer for the two conformers by ^1H NMR (see Appendix A for detailed characterization). This correlation supports the conclusion that the two different conformers have different T_d and were the cause of the feature in the TGA trace of **3**. It should be noted that this may have consequences on the use of **3** for TCNL as

total deprotection will only occur at temperatures above ~210 °C. However, since the majority of the material (80 %) pyrolyzes at temperatures as low as 150 °C, lower temperatures could still be used but will result in a reduced density of the functional group. Finally, the total mass loss over the two steps was approximately 40 %, which was the expected mass loss for the complete deprotection to amine.

2.4 Pyrolysis

TCNL is dependent upon control of thermal reactions, most notably decomposition reactions, on a surface. In order for this technique to be useful, an understanding of the thermal reactions possible on the surface was necessary. Carbamates possess two possible pathways of decomposition, yielding a possible mixture of two products, an amine or an isocyanate, as shown in Figure 10.^{26, 27} The isocyanate can then decompose further to yield a variety of compounds.^{26, 27} If the carbamate moiety is to be useful for producing reactive amine patterns, it is desirable that pyrolysis proceed primarily through the amine-producing decomposition pathway.

As a means of determining the pyrolysis products of the carbamate polymer ¹H NMR spectra of the material after pyrolysis were obtained by refluxing the carbamate

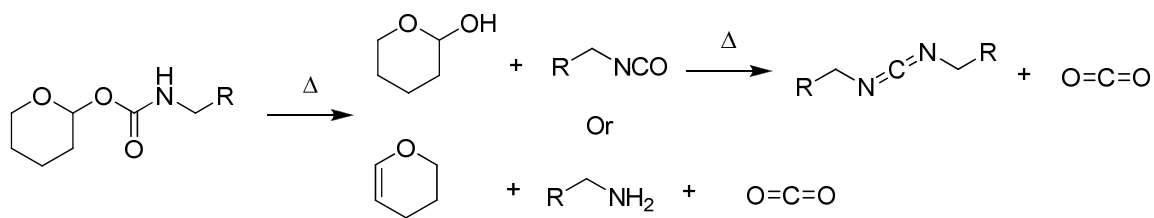


Figure 10: The most probable decomposition pathways of the THP-carbamate moiety.

polymer (**3**) in the high boiling point deuterated solvents nitrobenzene-*d*₅. Nitrobenzene has a boiling point of 211 °C which should be sufficient, according to the TGA data in Figure 9, to completely deprotect the carbamate without causing the polymer backbone to decompose. In order to simplify the study, a homo-polymer of the carbamate (**10**, synthesis described in Appendix A) was utilized. The structure and preferred pyrolysis products of **10** are depicted in Figure 11A. Approximately 50 mg of the carbamate homopolymer (**10**) was dissolved in 1.0 mL of nitrobenzene-*d*₅ and allowed to reflux for over an hour. A relatively large quantity of a black insoluble material formed. This black material was most likely due to the reaction of any amines formed with either formed isocyanates or the esters in the polymer backbone. The liquid portion of the mixture was pipetted off and any residual solid was removed by running it through a cotton plug.

The ¹H NMR spectra from both before and after refluxing are shown in Figure 11. A ¹H NMR spectrum of dihydropyran (DHP, **12**), one of the desired decomposition products, is shown in Figure 11d. These spectra and the presence of the insoluble black material indicate that a drastic change in **10** occurred upon heating and that DHP was the only soluble product present in measurable amounts. For DHP the peaks at 6.4 and 4.8 ppm should integrate for one H each and the peaks at 3.9, 1.9, and 1.8 ppm should integrate for two H each (Figure 11D). In the decomposition products the peaks at 3.9, 1.9, and 1.8 ppm integrate for 3 H when the peaks at 6.4 and 4.8 ppm are defined as one hydrogen (Figure 11C). The amount of noise in the baseline around these three peaks easily accounts for this discrepancy. The peak at around 2.7 ppm was due to water which is known to appear around this region in nitrobenzene-*d*₅.³¹

A

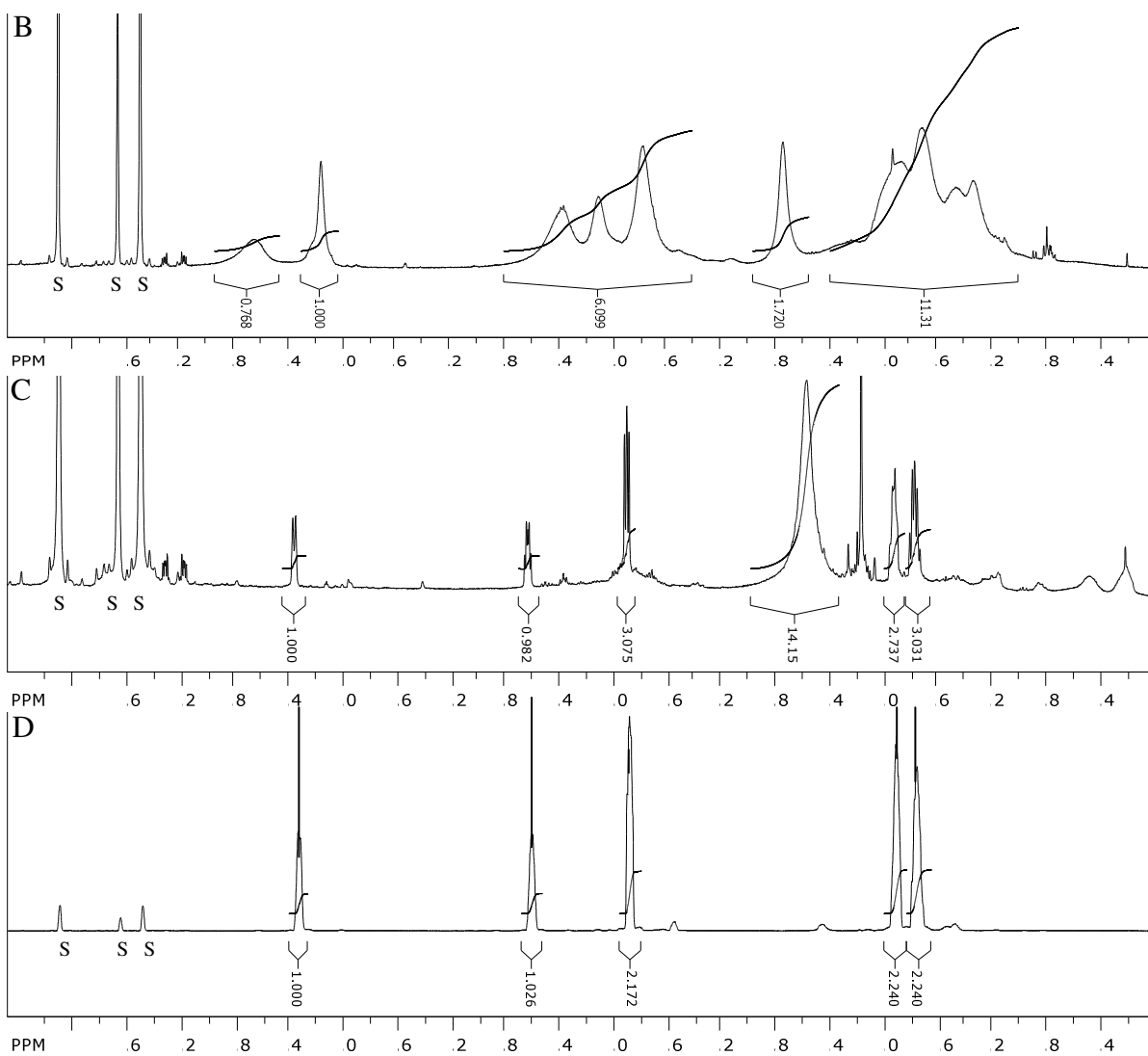
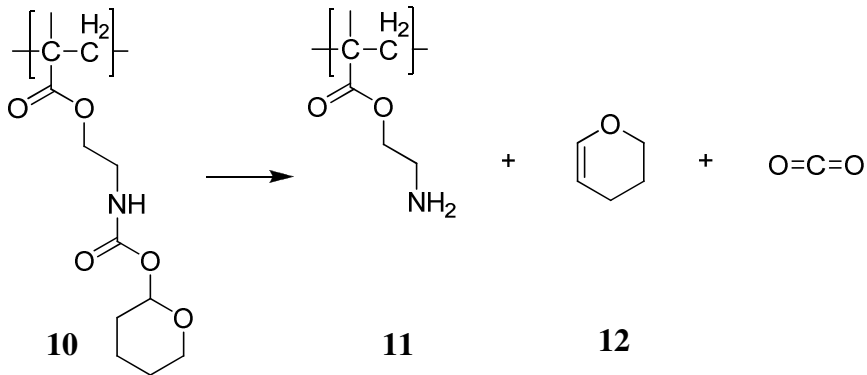


Figure 11: A) Structure and pyrolysis of **10**. ^1H NMR spectrum of **10** in nitrobenzene- d_5 both B) before and C) after refluxing. D) ^1H NMR of dihydropyran (DHP). S denotes solvent peaks.

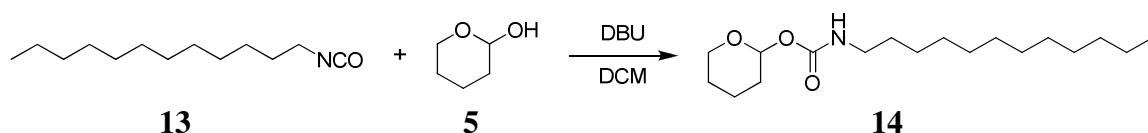


Figure 12: Synthetic pathway to tetrahydropyran-2-yl dodecylcarbamate.

As pyrolysis of the homopolymer (**10**) resulted in an insoluble residue, full characterization of the pyrolysis products was not possible. The only successfully isolated and identified material was DHP, which would seem to indicate that the amine does form to some extent (Figure 11). However, at high temperatures isocyanate can form other compounds, such as diimides accompanied by the loss of CO_2 .^{26, 27} These diimides can then react with the tetrahydropyran-2-ol formed, as depicted in Figure 10, to produce several different side products which would include DHP.^{26, 27} In order to obtain information on the functionality formed during decomposition a small molecule analog, tetrahydropyran-2-yl dodecylcarbamate (**14**) of the carbamate polymer was synthesized (Figure 12a). Once **14** had been synthesized, it had to be determined whether it would be a suitable model **10** in ^1H NMR pyrolysis studies. In order to be considered a suitable model several conditions had to be met. First, **14** must decompose in a similar manner to **10**. Second, the ^1H NMR spectra of the two expected pyrolysis products, dodecylamine and dodecylisocyanate, have to be distinguishable enough to allow for identification and quantification.

To determine whether **14** decomposed under similar conditions to **10** and **3** a TGA trace was obtained (Figure 13A). Unlike the TGA for **3** a two step mass loss was not observed for **14** before complete degradation of the material. Instead, only a single mass loss of 30 %, consistent with nearly complete conversion to the isocyanate (30.6 %),

was present. This single observed feature was, however, very close to where the 100 % mass loss occurred and any other features may have been obscured by the vaporization of any dodecylamine, boiling point (b.p.) of 247 – 249 °C, or dodecylisocyanate, b.p. of 157 - 161 °C, that had been formed. An isothermal TGA was obtained using the same temperatures as for **3** (Figure 9B) and a plot of the data can be seen in Figure 13b. The isothermal TGA seems to imply that the pyrolysis of **14** had two distinct steps, similar to the polymer **3**. The mass loss of the second step, however, never truly stabilized, unlike **3**, which maintained approximately the same mass while the temperature was held constant. This was most likely caused by the relatively low b.p. of the expected products relative to the temperature at which the polymer backbone of **3** would be expected to decompose. While the temperature held for this step of the isothermal TGA, 220 °C, was less than the b.p. of dodecylamine, 247 – 249 °C, the temperatures were close enough that some amount of the material would be expected to possess enough energy to volatilize, resulting in a slow mass loss. Since the temperature was greater than the b.p. of dodecylisocyanate, 157 – 161 °C, any that forms would be expected to volatilize instantly, resulting in 100 % mass loss. That total mass loss was not observed until temperatures above the b.p. of dodecylamine were achieved implies that the dodecylamine was the primary product, or that any dodecylisocyanate formed further decomposed into a diimide, a known biproduct^{26, 27} which would likely have a higher boiling point than the isocyanate (Figure 10). Such decompositions of isocyanate were not expected as they typically require at temperatures around 300 °C.^{26, 27}

Analysis of the percentage of mass lost during the isothermal portions of the TGA was inconclusive. If **14** decomposed fully into the isocyanate complete vaporization and

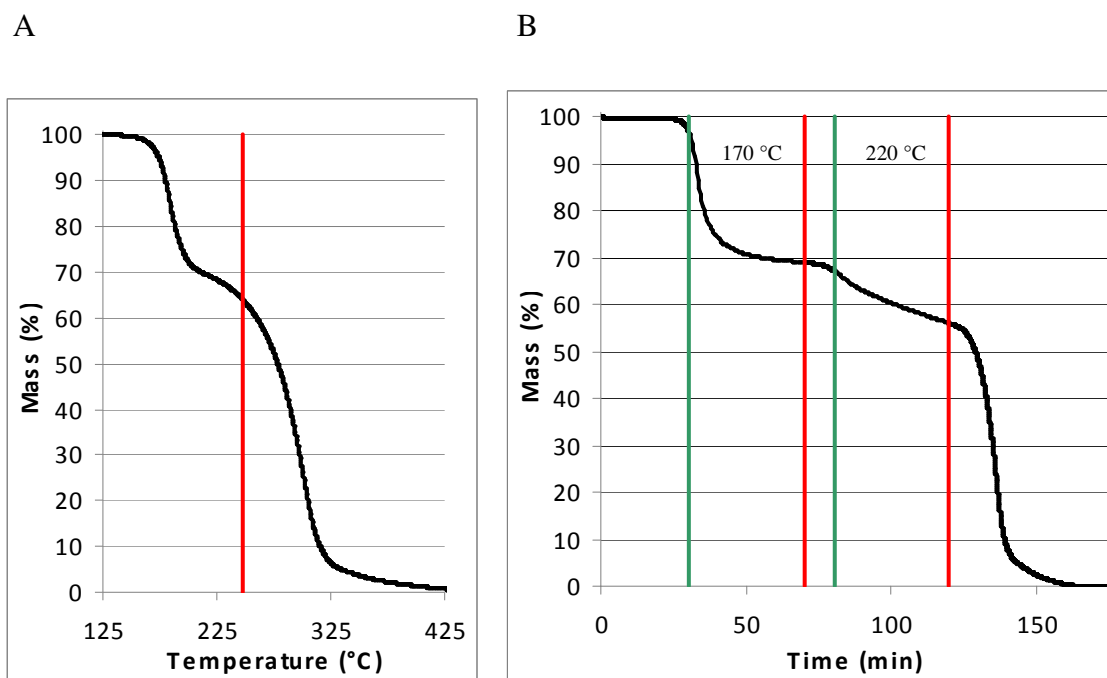


Figure 13: A) TGA of **14**, the line indicates the b.p. of dodecyl amine. B) Isothermal TGA of **14**, The lines indicate the times during which the temperature was held constant.

a mass loss of 100 % would have been expected without the mass ever having stabilized. If **14** decomposed fully into the diimide by way of dodecylisocyanate then a mass loss of 42 % would be expected. If **14** decomposed fully into the amine then a mass loss of 41 %, which is very similar to the value expected for a diimide, would be expected. While the isothermal TGA does not provide any conclusive information about which of the possible decomposition mechanisms was favored, it does behave similarly enough to the TGA of **3** to suggest that **14** is sufficiently analogous for further pyrolysis studies.

The next step before ^1H NMR studies of the pyrolysis of **14** could begin was to determine whether dodecylamine and dodecylisocyanate were both stable under the pyrolysis conditions and could be distinguished by their ^1H NMR spectra. As the structures of both of these compounds were very similar the differences in the spectra

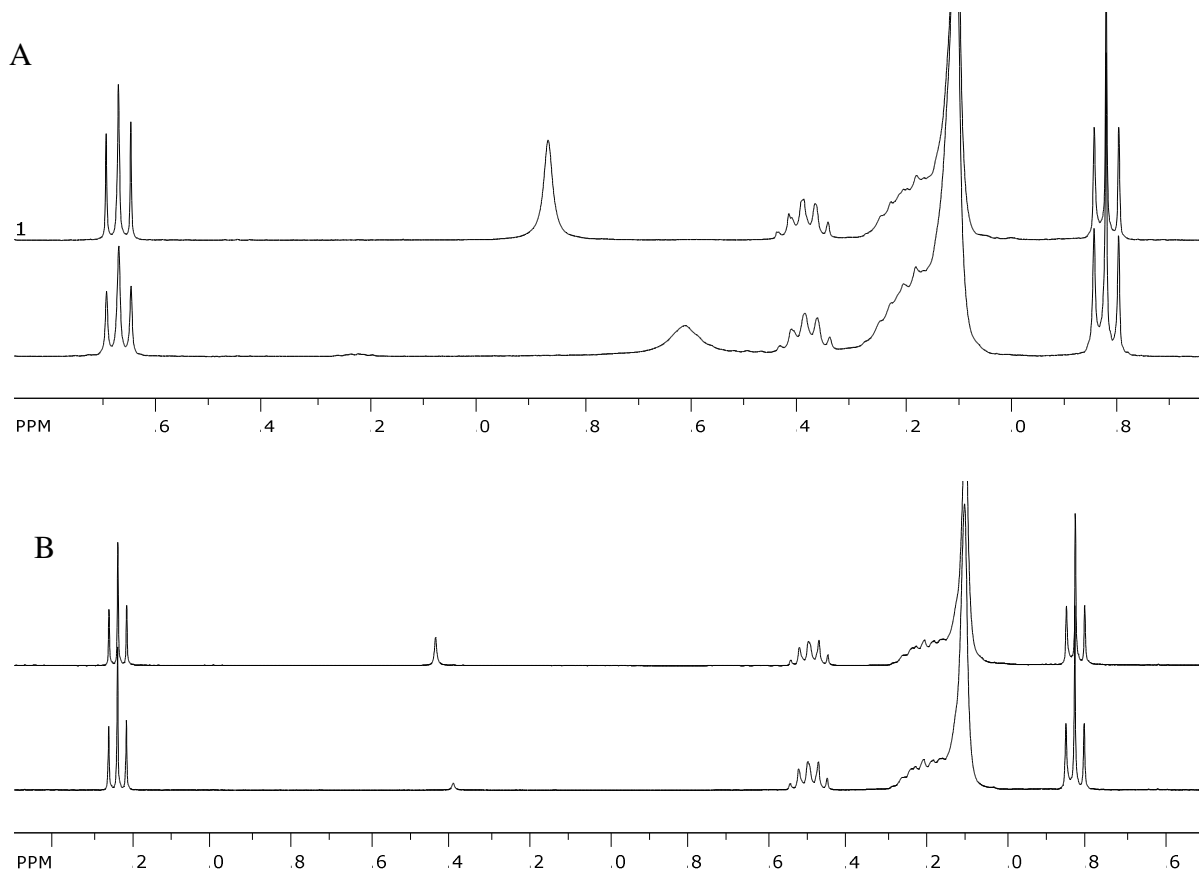


Figure 14: A) Dodecylamine and B) Dodecylisocyanate before (top) and after (bottom) refluxing in nitrobenzene.

were not expected to be large. The most likely protons for identification were the two alpha to the functional group as the frequency shift of a proton alpha to an isocyanate should be quite different from that of one alpha to an amine. Figure 14 demonstrates that this is indeed the case. The triplet for the alpha protons in the amine is found to be at slightly less than 2.7 ppm while the triplet in the isocyanate appears slightly above 3.2 ppm. This provides a rather significant 0.5 ppm difference between the two triplets, which should be sufficient for the identification of the products.

In order to test that the two expected pyrolysis products were stable at the temperature proposed for the experiment, 211 °C, a standard sample of each was refluxed

in nitrobenzene-*d*5. Spectra for both compounds before and after refluxing are shown in Figure 14. The peaks of interest, 2.7 ppm for the amine and 3.2 ppm for the isocyanate, were unchanged. In fact, the only observed change was in the singlet due to water.

¹H NMR spectra of the pyrolysis products of **14** were obtained in a similar fashion as for **10**. A solution of 25 mg of **14** was pyrolyzed by dissolving in 0.50 mL of nitrobenzene-*d*5 and then refluxing for approximately 15 minutes. As the solution cooled, a yellowish material began to solidify. Upon reaching room temperature, the majority of the solution had become a thick gel. Heating the sample to 80 °C melted the solid, releasing the solvent and allowing the solution to be analyzed by ¹H NMR. As was observed with **10**, several peaks that have been identified as dihydropyran were present (Figure 15a). The difference of chemical shifts between the spectra for the DHP standard and the pyrolyzed material was due to the DHP standard having been analyzed at room temperature while the pyrolyzed products were analyzed at 80 °C. The match in position and multiplicity was close enough that obtaining a ¹H NMR of the DHP standard at 80 °C was deemed unnecessary.

¹H NMR spectra of **14** were obtained at 80 °C both before and after refluxing and compared to the spectra of dodecylamine, dodecylisocyanate, and a relatively concentrated mixture of both (Figure 15B). The presence of a quartet at 3.3 ppm in the pyrolyzed sample indicates that some starting material was left over. The presence of remaining starting material was further supported by the presence of peaks at 6.0, 5.2, 4.0, and 3.6 ppm that possessed the same multiplicities as peaks at those locations in **14**. As the TGA implies the reaction should go to completion, the remainder of starting material after pyrolysis at 211 °C was unexpected. The quantity of remaining starting material

was estimated to be 8 % of the total material based on the integration of the quartet at 3.3 ppm relative to the combined integrations of the three signals at 2.7, 3.3, and 3.4 ppm.

Figure 15B shows a comparison of the material pyrolyzed at 211 °C to the dodecylamine and dodecylisocyanate. It is interesting that the peak at 2.7 ppm, which is believed to be due to the dodecylamine, is broad and difficult to assign a multiplicity. In the ¹H NMR spectrum of the dodecylamine standard this peak appeared as a very distinct triplet. Another oddity is the triplet that appears at 3.4 ppm in the spectrum of the pyrolyzed **14**. The only standard with a peak at this chemical shift is the mixture of dodecylamine and dodecylisocyanate, which would most likely have reacted together and formed didodecyl urea. However, the peak at 3.4 ppm from the mixture is a quartet, while the peak from the pyrolyzed material is a triplet. The peak from dodecylisocyanate is also a triplet. It is possible that these two observations could be explained by interactions of dodecylamine and dodecylisocyanate with both each other and the other species present in the solution, such as DHP or the remaining amount of **14**. This could also explain the broadening of the peaks and could result in a shift of the isocyanate peak to a more deshielded position. Also, the concentration used for the pyrolysis was much lower than that used to create the mixed standard, making a chemical conversion to the urea less likely to occur.

The three peaks at 2.7, 3.3, and 3.4 ppm (thought to be dodecylamine, **14**, and dodecylisocyanate respectively) are well enough resolved that a comparison of their areas can be made. The integration of the peak at 3.4 ppm was set to one and the ratio of amine to isocyanate was found to be about 3.6 to 1 (Figure 15B). For the purposes of TCNL this ratio should be as high as possible. In the worse-case scenario all of the

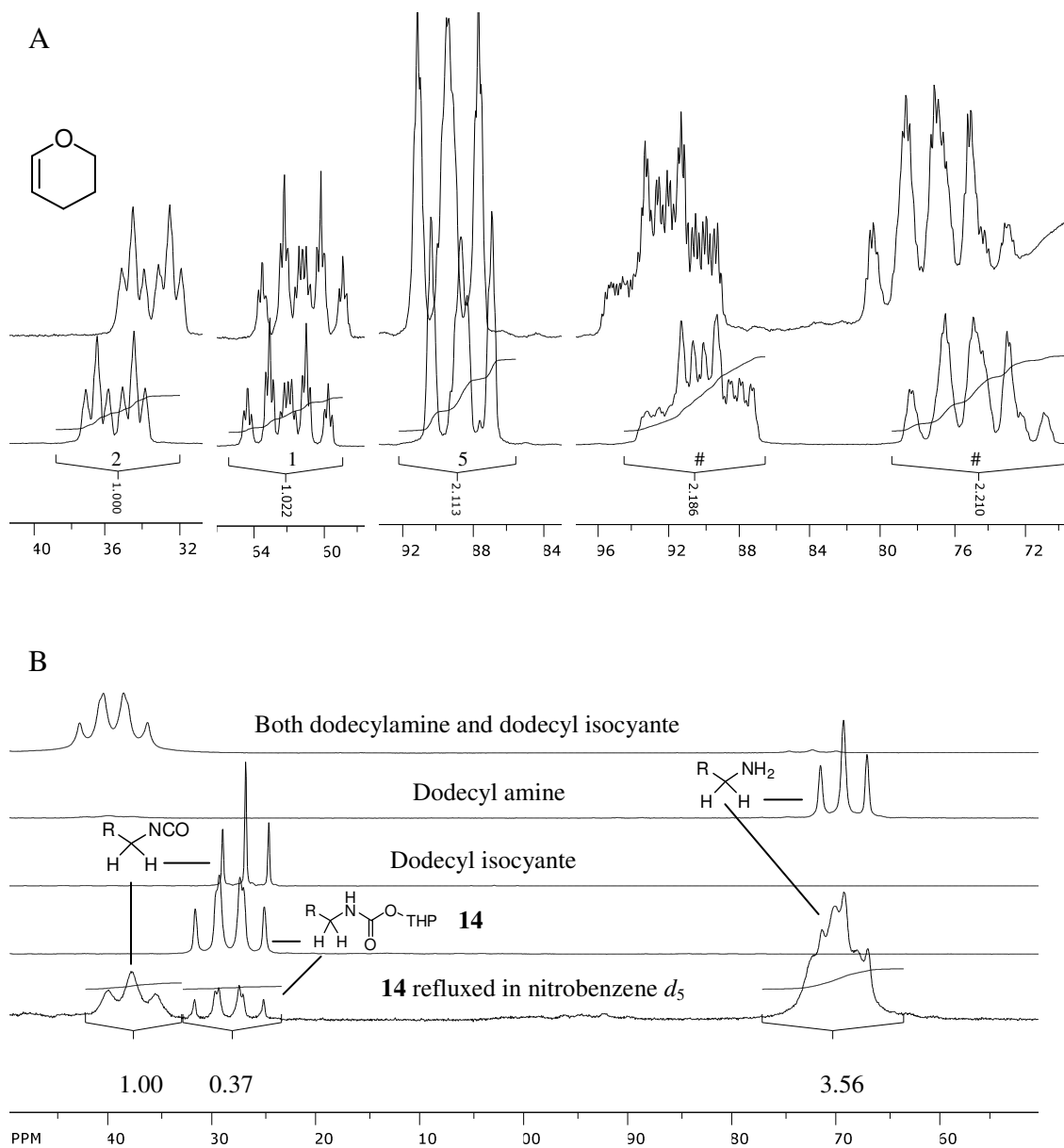


Figure 15: A) Comparison of DHP (bottom) to **14** pyrolyzed in nitrobenzene- d_5 (top). B) ^1H NMR spectra of pyrolyzed **14**, (bottom), the original material, and the most likely products. All spectra except for that of DHP were collected at 80 °C.

isocyanate would react with the available amine groups. Assuming the material decomposes in a similar fashion in the solid state, then such a scenario would result in only 52 % of the available amines being available for post-modification. This number takes into account the 8 % undecomposed material. If we assume that the ratio of amine to isocyanate would have been the same had the reaction gone to completion then the worst case scenario results in 56 % of all deprotections yielding a free amine. The best case scenario, where the isocyanate does not react with any of the amines, would result in 78 % of all deprotections yielding the amine. For many applications, such as patterning of proteins onto a surface, the size of the protein is significantly larger than the binding sites, reducing the necessity of a high-density of reactive groups. As over 50 % of the deprotections will result in a viable amine, polymer **3** should function adequately for such applications. Should a higher-density of amines be needed, a method of increasing the amine to isocyanate ratio would be necessary. Such a feat could possibly be accomplished by selecting a different functional group.

2.5 Summary

The proposed carbamate containing copolymer (**3**) was successfully synthesized and characterized. TGA showed that **3** possessed two distinct T_d . One starting around 150 °C and accounting for 80 % of the mass loss, and a second starting around 210 °C that accounted for the last 20 %. The total % mass observed was approximately 40 %, which is in good agreement with the expected mass loss for the formation of a primary amine (38.4 %). Pyrolysis of the material in nitrobenzene- d_5 demonstrated that **3** preferentially decomposed into a primary amine upon pyrolysis and it was assumed that

the material would behave similarly in the solid state. The polymer **3** has been demonstrated to possess the necessary chemical properties for use with TCNL in the formation of amine patterns. Before patterning can be attempted, however, films of **3** must be prepared and analyzed.

CHAPTER III: DEVELOPMENT AND CHARACTERIZATION OF FILMS

3.1 Introduction

The production of patterns of amine using polymer **3**, synthesized and characterized in Chapter II, using TCNL requires that films of the polymer be produced first. These films will provide the surface that the AFM tip will pyrolyze and should ideally meet certain requirements. First, the surface should be relatively smooth. Second, the material should require very little processing in easily obtainable conditions. Finally, the chemical reactions built into the design of **3**, thermal formation of an amine and cinnamate crosslinking, must still occur in the film. Spin coating was the processing method selected. Spin coating is a simple, inexpensive method of creating films of varying thicknesses under ambient conditions.

3.2 Preparation of Films

Films of polymer **3** were prepared on either glass or silicon substrates by spin coating from a solution of **3** in cyclohexanone. Various concentrations of the polymer in cyclohexanone were spun at various speeds, as reported in table 1. For most of the following studies a concentration of 20 mg / mL and spin speed of 1000 revolutions per minute (RPM) was used and yielded films with a thickness of 75 ± 5 nm. The ketone in the solvent, cyclohexanone, would be expected to bind any amines that may have formed from undesired deprotection during processing, forming a Schiff base.³² This could act as a protective measure against such accidental deprotection. Upon heating the contact angle of the polymer film was typically reduced from $71 \pm 3^\circ$ to $56 \pm 3^\circ$ for a difference

Table 1: Typical thicknesses of polymer films based on concentration (mg / ml) and spin speed (RPM). Determined by stylus profilometry

Concentration	1000 RPM	1500 RPM	2000 RPM
50 mg / mL	N/A	N/A	150 ±5 nm
20 mg / mL	75 ±5 nm	N/A	N/A
10 mg / mL	60 ±5 nm	30 ±5 nm	N/A

of $15 \pm 4^\circ$. A reduction in the contact angle of the film was expected as the pyrolysis from a carbamate to an amine should increase the hydrophilicity of the surface.

The ester polymer (poly(tetrahydropyran-2-yl methacrylate)-poly(methyl 4-(3-propoxymethacrylate) cinnamate)) that had been previously studied^{9, 13} had been observed to occasionally delaminate from the surface during processing, especially during washing. This delamination problem was also observed for sample films created from **3**. Delamination occurred during either chemical modification of the patterned functionality or the subsequent washing steps. A method to covalently crosslink the polymer to the substrate was sought as a means to prevent delamination. It has been shown that monolayers of 4-(3-(chlorodimethylsilyl)propoxy)benzophenone (**17**) can be used to covalently bind thin polymer films to SiO₂ surfaces.³³ This was accomplished by taking advantage of the $n - \pi^*$ transition of benzophenone upon irradiation at around 350 nm. The resulting radical on the oxygen of the carbonyl abstracts a hydrogen from the C-H bond of an sp³ hybridized C and then to binds the resulting carbon radical.^{33, 34} Even though benzophenone can generally only bind film within the immediate vicinity of the substrate,³³ the cinnamate should, after crosslinking, form a covalently bound network attached directly to the surface through **17**.

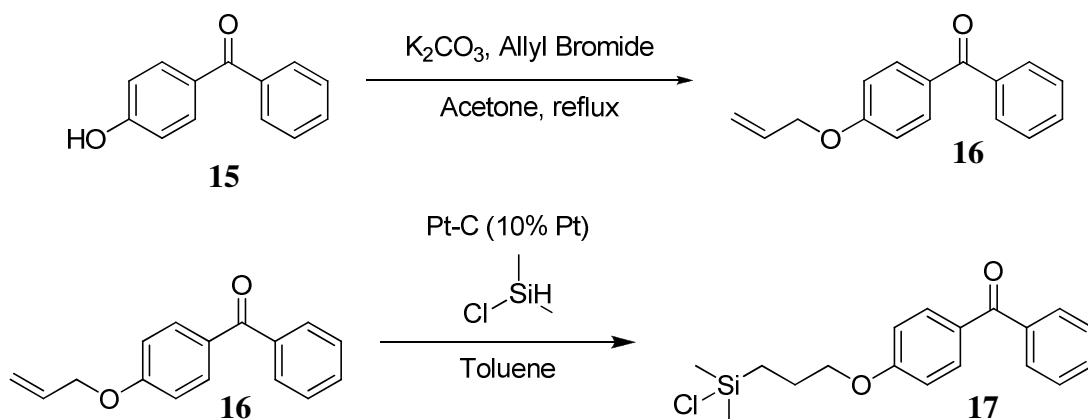


Figure 16: Reaction scheme for the synthesis of **17**.

The synthesis of **17** was achieved through a reported procedure (Figure 16).³³ The first step involved the Williamson ether synthesis of allylbromide with 4-hydroxybenzophenone to form allyloxy benzophenone (**16**). The final product was then synthesized through the hydrosilylation of the double bond using a platinum catalyst on activated carbon (10% Pt). The product contained a small amount of contaminants, presumed to be hydrolyzed silanes that subsequently condensed. As further purification would have been difficult to perform without risking the complete loss of the product, and only the desired product should contain a reactive silane and therefore be able to bind to the substrate, the material was used as is. No further delamination has been observed since the incorporation of monolayers of **17** on glass substrates before the creation of any polymer.

Direct evidence for the effectiveness of the benzophenone monolayer has also been obtained by binding **17** onto both glass and silicon surfaces. The observed contact angle of the substrates after functionalization with **17** could be used as a rough indicator of the quality of the monolayer formed. A typical contact angle for a monolayer of **17**

had been found to be from 60 – 70 ° which was consistent with the contact angle of monolayers made from a phosphonic acid analogue to **17**.³⁵ Polymer films were created on both one glass and one silicon wafer that had been modified with **17** and one glass and one silicon wafer that had not been modified. The films were crosslinked by exposure to 300 nm radiation for 40 minutes and then sonicated in dimethylsulfoxide (DMSO) for 15 minutes. After sonication the wafers were visually inspected for the presence of the polymer film. The glass slide that had been treated with **17** was observed to be hydrophobic, while the glass slide that had not been treated was hydrophilic. Also, scratches could be made on the benzophenone-treated slide using a flat, metal spatula, while the untreated slide could not be scratched by the same spatula. Scratching the side of the slide that had not been coated with a polymer film did not create any visible marks, indicating that the scratches observed could only be made when a film of **3** was present. The silicon wafer that had been treated with **17** was observed to be hydrophobic while water wetted the untreated surface. Also, polymer films on silicon substrates were visible as a dark brown color with blue, iridescent edges. These traits were observed on the silicon wafer that had been treated with **17** but not on the silicon wafer that had not been treated with **17**. Finally, only the silicon wafer treated with **17** could be marked by scratching with the flat side of a spatula. It is of interest to note that the monolayer of the specific glass slide used for this experiment had a contact angle of only 50 %, indicating a poor monolayer. The sample was used despite this in order to determine if the **17** would still serve its function when a less than ideal monolayer was present. The contact angle for the silicon wafer was consistent with the formation of a good monolayer, as

described above. These observations indicate that the addition of a benzophenone monolayer successfully prevented the loss of the film due to delamination.

3.3 Characterization of Films

The system being developed involves three chemical reactions. The first reaction was the binding of the monolayer of **17** to the polymer film after exposure to 350 nm radiation. The second reaction was the crosslinking of the cinnamate portion of polymer **3**. The final reaction was the deprotection of the carbamate moiety upon heating. Evidence that the desired chemical reactions occurred was obtained through the use of a technique called specular reflectance Fourier transform infrared (FT-IR) spectroscopy. This spectral technique analyzes thin films by passing an infrared beam through the film at a fixed angle to reflect off of the substrate, providing a longer path length through the material and allowing analysis of films on substrates that are not transparent to infrared light. The signal strength obtained for any given film depends on the angle of incidence of the light, the reflectance of the substrate at that angle, and the thickness of the polymer film.³⁶

Several films of **3** on glass substrates that had been modified with **17** were prepared and analyzed using an angle of incidence of 16 °. These samples yielded too low a signal-to-noise ratio to be accurately analyzed, so several new samples were prepared using silicon as the substrate. Silicon has a higher reflectance at the angle of incident used than glass does, resulting in a better signal to noise ratio.³⁶ Purging the FT-IR sample chamber with a flow of N₂ further improved the spectrum quality by reducing the noise due to water to acceptable levels. It should be noted that this technique is not

sufficiently sensitive to provide any information on the reactions of the monolayer of **17** as the signal from this layer would be too small to observe, especially when compared to the signal from the polymer film.

The first of the observable reactions studied was the crosslinking of the cinnamate group, shown in Figure 17A. The cinnamate moiety of the polymer films were crosslinked 1700 cm^{-1} .³⁷ The small peak just above 1600 cm^{-1} , marked by the arrows in Figure 17B, is thought to be due to the non-aromatic double bond in the cinnamate. The loss of this peak upon irradiation is a strong indication that the desired crosslinking has

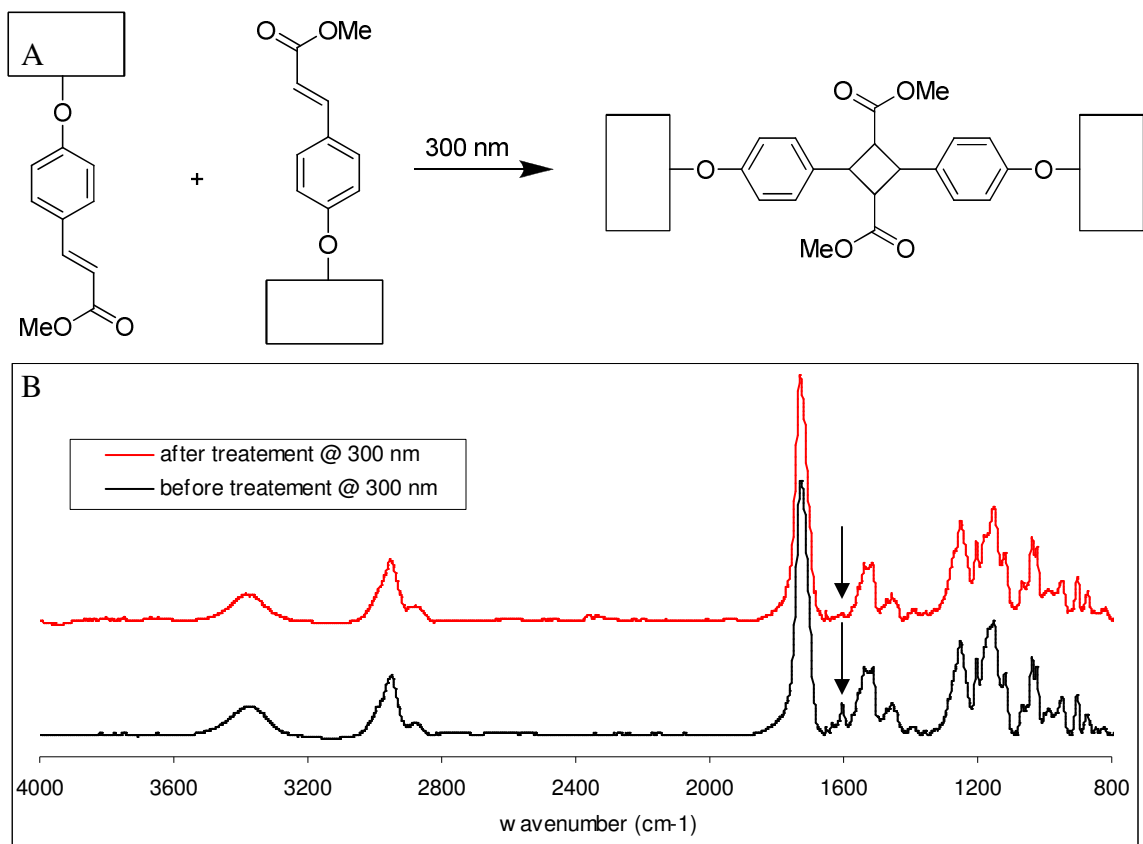


Figure 17: A) Scheme of the photocrosslinking reaction of the cinnamate moiety in the polymer films. B) FT-IR spectra of a carbamate film both before (black) and after (red) irradiation at 300 nm. The arrows show the disappearance of the peak associated with the double bond stretching mode in the cinnamate ($\sim 1606\text{ cm}^{-1}$).

occurred. The spectra in Figure 17B were obtained after a long period of ultraviolet (UV) exposure and only demonstrate the crosslinked and uncrosslinked states. In order to optimize irradiation conditions spectra of the change of this peak with respect to time would be useful. Also, the monolayer of **17** must be exposed to UV radiation as well (354 nm for one hour). It would be ideal if these two photo-treatment steps can be combined together, especially considering there was only a 56 nm difference in the wavelengths used.

Specular reflectance FT-IR spectra and UV absorption spectra were obtained for the polymer film for different times of ultraviolet exposure. UV spectra were obtained using glass substrates. UV and FT-IR spectra before and after exposure to 354 nm irradiation for one hour are shown in Figure 18A. It is clear from these spectra that exposure to 354 nm radiation does cause the cinnamate to crosslink, although slowly. While the cinnamate does not absorb significantly at this wavelength, it is likely that the emission band of the lamp used had sufficient overlap with the absorption band of the cinnamate to activate the crosslinking. Figure 18B shows the UV and FT-IR spectra for polymer films that were exposed to 354 nm radiation for 1 hour and then to 300 nm radiation for up to 35 minutes. The spectra were taken at various intervals during the photo-treatment and both spectra indicate the peak for the cinnamate disappeared within 20 – 25 minutes. Figure 18C shows the UV and FT-IR spectra for polymer films that were only exposed to 300 nm light. Spectra are only reported for the first 35 minutes as this was more than sufficient time for complete crosslinking. The peak at 280 nm in the UV continued to grow for the entire 60 minutes during which the spectra were taken, though the rate of growth slowed after approximately 40 minutes. Both spectra indicate

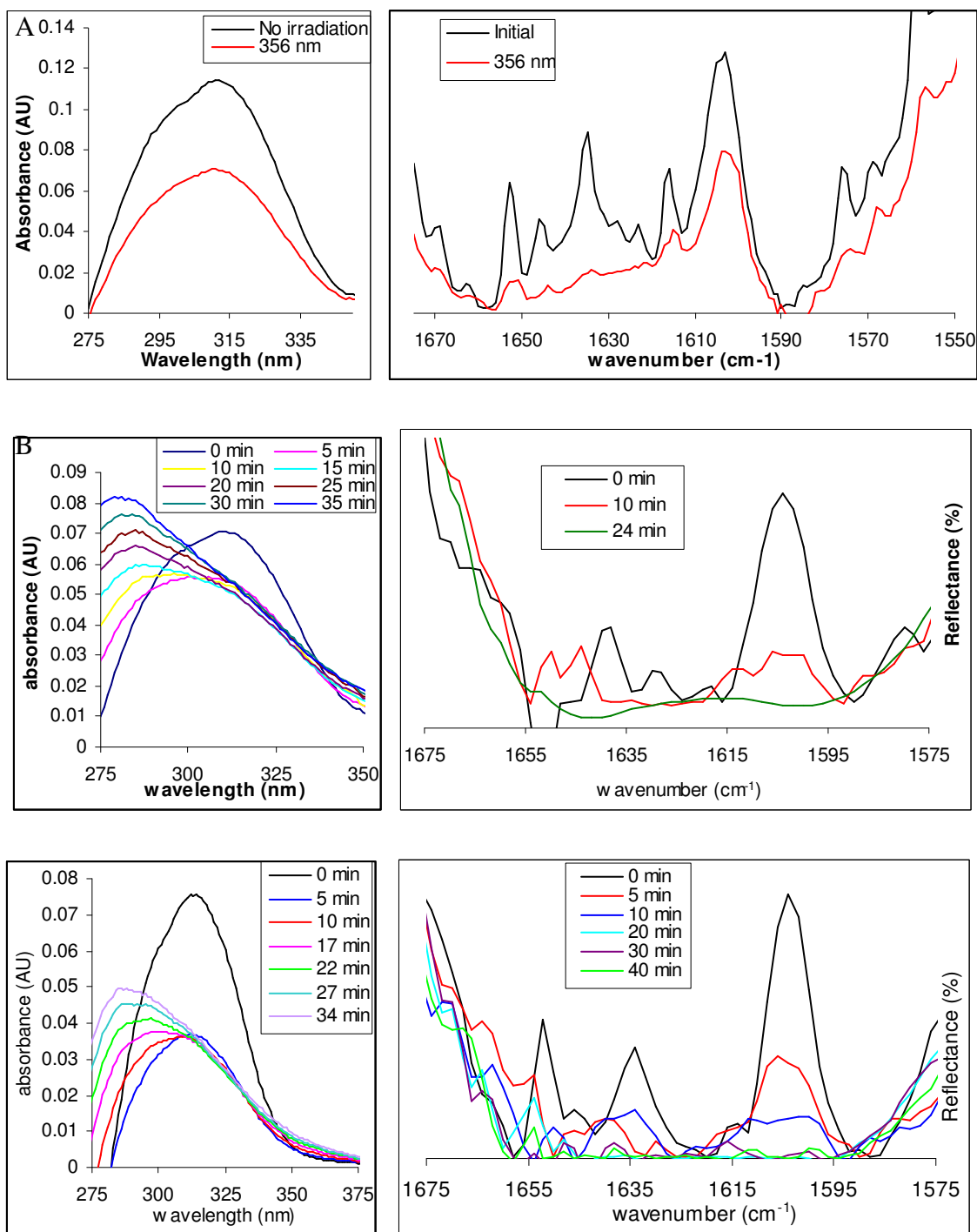


Figure 18: A) UV and FT-IR spectra of films of **3** before and after exposing to 354 nm radiation for 60 minutes. B) UV and FT-IR spectra of films exposed to 354 nm for 1 hour and 300 nm for varying times. C) UV and FT-IR spectra of films exposed only to 300 nm for varying times.

that crosslinking was completed after approximately 20 minutes, nearly the same as that for the samples that had been irradiated at 354 nm for 60 minutes prior to 300 nm irradiation.

As irradiation at 354 nm only resulted in relatively slow crosslinking of the cinnamate group, it was unlikely that this wavelength could be used to develop a single-step photo treatment. If a simplification of the processing performed on the films of **3** was going to be possible it would require that the monolayer of **18** binds to the polymer when irradiated by 300 nm light. As benzophenone is known to possess a reasonable absorption at 300 nm, it seems likely that this wavelength should initiate this reaction.³⁸ The test of this was discussed above in section 3.2. To summarize, one glass slide and one silicon wafer were modified with **17**. Both of these samples were then coated with a polymer film along with one glass slide and one silicon wafer that had not been modified with **17** and all of the films were irradiated at 300 nm for 40 minutes. The reason the slides were exposed for 40 minutes despite the spectra in Figure 18 showing that crosslinking completes in half that time was to ensure the monolayer of **17** had sufficient UV exposure to bind the film. When, after irradiation, these samples were sonicated in DMSO the polymer film was only found on the surfaces that had been treated with **18**. These results indicate that a single irradiation step at 300 nm should be sufficient for film processing.

Now that the crosslinking of the polymer film had been demonstrated, it was necessary to determine what chemical changes occurred upon heating the film. The desired reaction is shown in Figure 19. This decomposition should be observable by FT-IR as a carbonyl group would be lost and a primary amine would be formed. Also a large

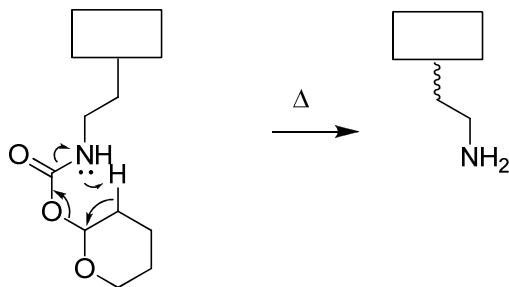


Figure 19: Pyrolysis of the carbamate moiety.

number of the sp^3 hybridized C – H bonds would be lost. If the undesired decomposition occurs instead, resulting in an isocyanate (as discussed in Chapter II), then it should be readily identifiable as isocyanates have a strong, distinctive peak that appears between 2200 and 2300 cm^{-1} .

Four films of **3** were prepared on silicon wafers and crosslinked. Each of the samples was then analyzed by specular reflectance FT-IR and then heated to either 120, 150, 180, or 210 °C and again analyzed by specular reflectance FT-IR spectroscopy. Upon heating the films heated to 150, 180, and 210 °C changed color while the film heated to 120 °C remained a dark brown. Figure 20 shows a comparison of the FT-IR spectra of the thin films. The sample heated to 120 °C showed very little change relative to the unheated film. This was expected as the TGA for **3** (Figure 10, Chapter II) does not indicate any mass loss until approximately 150 °C. The samples heated to 180 and 210 °C both changed significantly. The most notable change was the reduction in signal from the carbonyl stretch at 1720 cm^{-1} . It was not expected that the carbonyl peak would disappear entirely as **3** contains several other carbonyl moieties that should be unaffected by the thermal treatment. Also of particular interest was the near total loss of the N – H

stretching peak at approximately 3400 cm^{-1} . The loss of this feature is most likely a result of hydrogen bonding between the amine hydrogens and the oxygen atoms present in the polymer film. The steric hindrance of the THP group might prevent such hydrogen bonds from forming before deprotection. The appearance of a new peak at approximately 1650 cm^{-1} is consistent with the N – H bending of an amine.³⁷ It is interesting to note that this peak is not present in the sample heated to $150\text{ }^{\circ}\text{C}$. According to the TGA data discussed in Chapter II, decomposition began around $150\text{ }^{\circ}\text{C}$, so this temperature may not have been sufficient to deprotect a significant portion of the polymer in the time allowed. Finally, the band due to the C-H stretch at just below 3000 cm^{-1} was reduced in intensity upon heating, as was expected.

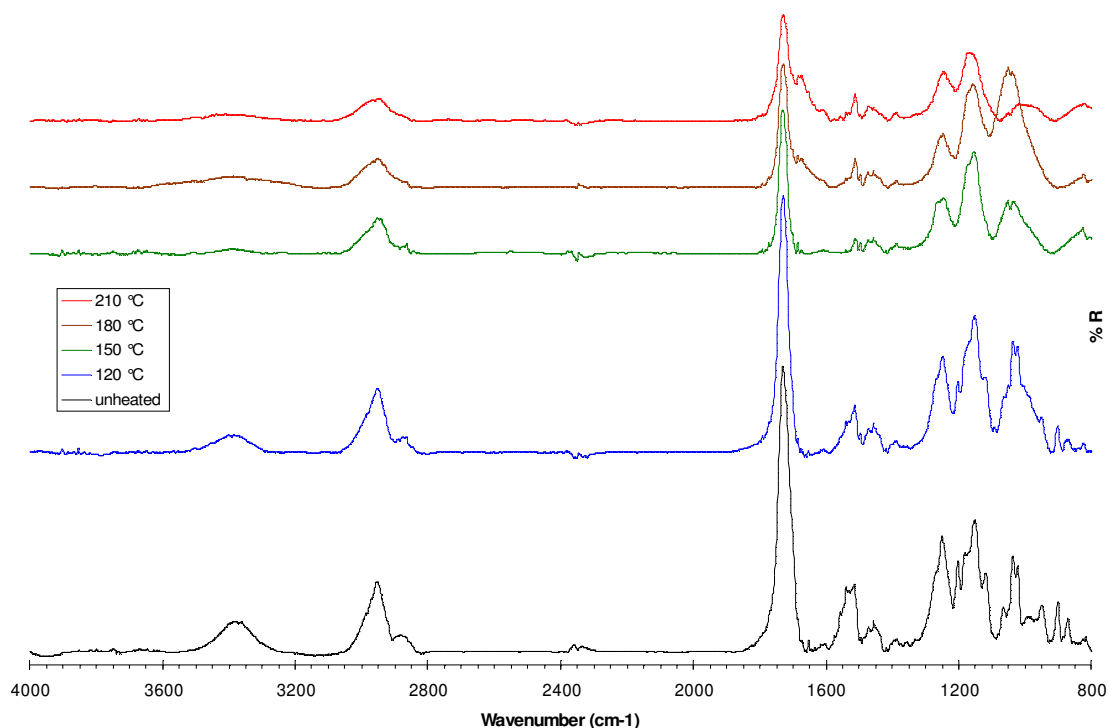


Figure 20: FT-IR of spectra of carbamate films heated to different temperatures.

With the exception of the loss of the N-H stretch at 3400 cm^{-1} , each of the observed changes was more significant in the samples heated at higher temperatures. This is, again, consistent with the TGA trace for **3** as only the sample heated to $210\text{ }^{\circ}\text{C}$ has a high enough temperature for complete deprotection. It does not seem that a significant amount of isocyanate formed as there was no peak observed between 2200 cm^{-1} and 2300 cm^{-1} (the feature observed at 2340 cm^{-1} was from fluctuations in the concentration of atmospheric CO_2 that the N_2 purge of the sample chamber was unable to eliminate). In general, the spectra in Figure 20 indicated that the deprotection of the polymer film only appreciably occurs upon heating to at least $180\text{ }^{\circ}\text{C}$ and that a temperature greater than $210\text{ }^{\circ}\text{C}$ results in higher percent decomposition. The FT-IR spectra also imply that the main decomposition product was the primary amine and not the isocyanate.

3.4 Summary

Thin films of the **3** have been produced and characterized. The effectiveness of monolayers of **17** at preventing the delamination of films of **3** was demonstrated. The crosslinking properties of the cinnamate have been better characterized and a one-step photo-processing method for the activation of both the benzophenone and the cinnamate has been developed. The films have been shown through FT-IR spectroscopy to undergo the pyrolysis reactions necessary to be compatible with the patterning of primary amines by TCNL. The next step is to demonstrate the ability to post-modify the surface and then use TCNL to create chemically reactive patterns.

CHAPTER IV: PATTERNING OF PRIMARY AMINES AND PPV

4.1 Reactive Amine Patterns

4.1.1 Introduction

The characterization experiments of the thin film of **3** discussed in Chapter III indicate that these films possess the properties needed to be a viable candidate for use with TCNL. The carbamate functionality in the film has been shown to decompose to form primary amines as the major decomposition product upon heating at temperatures low enough to prevent damage to the film. Successful incorporation of these films with the technique of TCNL requires that they first demonstrate the ability to be chemically modified after heating. Once that has been shown, micron scale patterns will be made to test the specificity of post-modification for the patterned areas.

4.1.2 Bulk Test of Fluorescent Procedure

The ability of the deprotected film to be modified after deprotection has yet to be demonstrated. To this end several samples of the bulk film were heated to 180 °C and then exposed to a fluorescently tagged protein. The protein selected for this study was fibronectin modified with the fluorescent tag Atto 488 by Vamsi Kodali (School of Physics, Georgia Institute of Technology). Glutaraldehyde, a homobifunctional crosslinking agent commonly utilized in biological studies,²⁴ was used to bind the fibronectin to the polymer. The general scheme for this study can be found in Figure 21. Both heated and unheated films of **3** were prepared and half were treated with

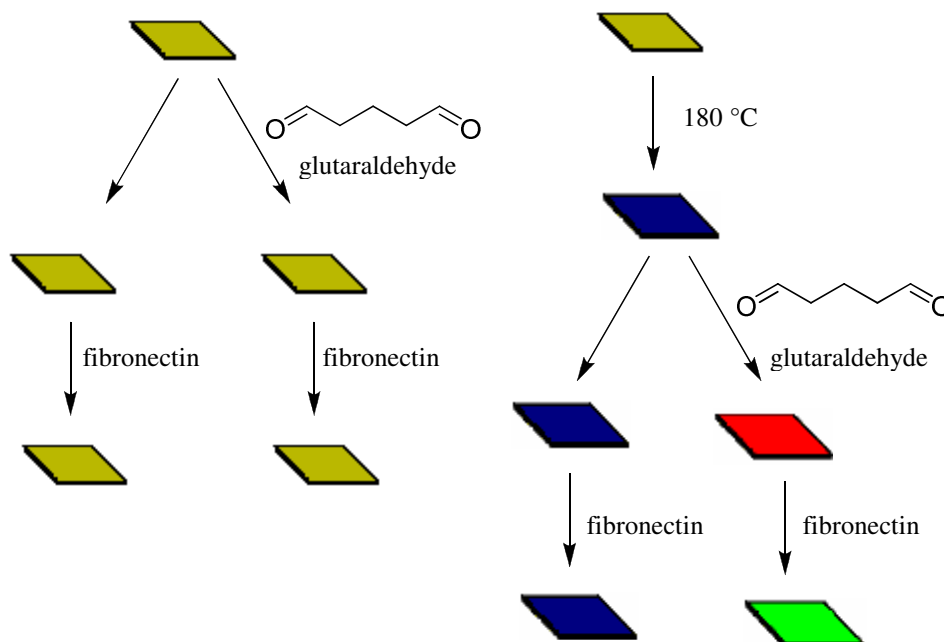


Figure 21: Scheme for the preparation of bulk fluorescence samples.

glutaraldehyde. All of these slides were then treated with fibronectin and the resulting fluorescence intensities were measured and are shown in table 2. These intensities indicate that the fibronectin adheres preferentially to the heated surface that has been treated with glutaraldehyde, a result consistent with successful post-modification of the polymer film. It should be noted, however, that the heated sample that had not been exposed to glutaraldehyde still possessed a fluorescent peak just over twice the polymer control. That a primary amine can adhere proteins was no surprise as there are very few substances that resist protein adhesion.² It was also observed that the unheated polymer that had been exposed to glutaraldehyde also possessed an increased fluorescence, though not as strong as either of the heated samples. This represents the affinity of undecomposed **3** to bind glutaraldehyde. Such non-specific binding is likely to reduce

Table 2: Average fluorescence (in arbitrary units) of polymer films prepared according to the scheme in Figure 21.

Sample	Average Fluorescence (a.u.)
180 °C w/ glutaraldehyde	18000
180 °C (no glutaraldehyde)	5900
Unheated w/ glutaraldehyde	4400
Unheated (no glutaraldehyde)	2700
Substrate	1300

the contrast obtainable with this system through TCNL and methods of reducing non-specific binding are desirable.

4.1.3 Micropatterns

The ability of the polymer films discussed in chapter III to be post modified having been established, the next step was to begin creating micrometer scale patterns. Using a resistively heated AFM tip a 4×4 matrix of $10 \mu\text{m}$ squares were patterned by Debin Wang (School of Physics, Georgia Institute of Technology) onto two separate films on glass. One sample was then conjugated to the fluorescent fibronectin (Figure 22A) and the second film was conjugated with fluorescein isothiocyanate (FITC) (Figure 22B). The left side of the squares in Figure 22A tends to be brighter than the right side. This was caused by a quirk in the AFM software that caused the heated AFM tip to pass over the left side twice and the right side only once. This programming glitch has since been removed. For several of the squares patterned in Figure 22A, however, the left side was darker than the right. The topmost square second from the left exhibited this inverse behavior. The most likely explanation for this observation was that the packing of the

fluorescent molecules was close enough to cause concentration quenching. Concentration quenching is a known phenomena that results in the loss of fluorescence through Förster non-radiative energy transfer.³⁹ The range of differences, however, does indicate a problem with the repeatability of patterning. In Figure 22B the center of each square developed a single bright spot from where the AFM tip first came into contact with the polymer film. This was caused during the descent of the AFM tip, which had been preheated away from the surface. As the hot tip descended towards the center of the square it began to heat the surface, resulting in a longer amount of time to pyrolyze then the rest of the surface. The patterning program has since been modified to prevent this. Variations in fluorescence intensities again points to a repeatability issue. Friction measurements taken after patterning but before post modification provided supported evidence that successful conversion to an amine had occurred (Figure 21C). These preliminary results demonstrate the effectiveness of the polymer films developed to create patterns through TCNL. Further work is needed, however, to increase the reproducibility and determine the resolution limits possible.

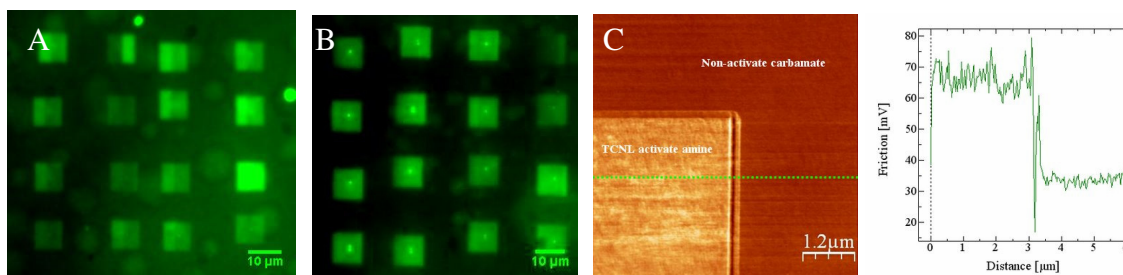


Figure 22: 10 μm squares patterned by TCNL and conjugated to A) fluorescently modified Fibronectin or B) fluorescein isothiocyanate FITC. C) Friction measurements of a patterned square from A) after TCNL but before protein conjugation.

4.2 Patterns of Polyphenylene Vinylene (PPV)

4.2.1 Background

Highly conjugated polymers, such as polyphenylene vinylene (PPV) and polyacetylene, have received a great deal of attention due to their potential conductive properties.⁴⁰⁻⁴³ These properties have potential applications in photovoltaics and organic light emitting diodes as a replacement for the inorganic semiconductors that see much current use.⁴¹ The high degree of pi-conjugation that provides these useful chemical properties also tends to make any long-chained polymers highly insoluble and hard to work with.⁴² To overcome these issues, several methods of soluble polymer precursors have been developed.⁴⁰⁻⁴³ One such method uses the pyrolysis of a sulfonium salt precursor to produce PPV (Figure 23). As the precursor salt is water soluble high-molecular weight films can be made through spin coating. These films are known to convert to PPV upon heating to 250 °C.⁴³ By taking advantage of this thermal conversion, TCNL should be able to create small scale patterns of conductive polymer.

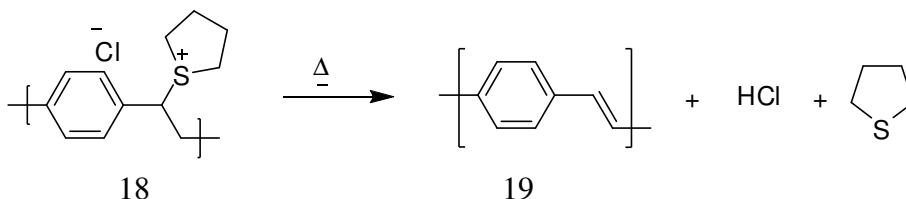


Figure 23: Thermal conversion of **18** into PPV (**19**).

4.2.2 Procedures

Several films of **18** on glass slides were created by spinning either a 0.125 % or a 0.0833 % solution of **18** in water. The glass slides were washed by sonicating in ethanol and then placing the substrates in piranha solution (75 % of concentrated H₂SO₄ / 25 % of 30 % H₂O₂ in water) heated to 50 °C for 30 minutes. To test the effect of polymer concentration and spin speed four glass slides were coated with 0.125 % solution, two were then spun at 1000 RPM and two were spun at 2000 RPM. Four other glass slides were coated with 0.0833 % solution. Two each were spun at 1000 and 2000 RPM. The slides were then exposed to long-wavelength UV radiation, causing the films to fluoresce due to a small amount of conjugation that occurs during synthesis,⁴² allowing them to be visually observed. The observations made are noted in table 3. The brightest sample with an even coating, spun at 2000 RPM from a 0.125 % solution, was given to Yueming Hua (School of Chemical and Biochemical Engineering, Georgia Institute of Technology) to be patterned. After patterning the slide was imaged using a fluorescent microscope. Figure 24 shows the image of the 5 μm × 10 μm pattern created in the PPV film. This demonstrates that TCNL can create patterns in the tetrahydrothiophenium salt, though the fluorescence could be a result of the formation of oligophenylene vinylene instead of full conversion to PPV.

Table 3: Observations of slides coated under different conditions

Polymer Concentration	Spin Speed (RPM)	Observations
0.125 %	1000	Uneven coating with only spots of polymer
0.125 %	2000	Bright, even coating
0.0833 %	1000	Dim, even coating
0.0833 %	2000	Even coating in the center, spots at the edge



Figure 24: The word PPV ($5\ \mu\text{m} \times 10\ \mu\text{m}$) written through the thermal conversion of poly(p-xylene tetrahydrothiophenium chloride) onto PPV. Image taken with a $60\times$ oil objective and a CCD camera with an exposure time of 9.08s using a neutral density filter - 8 (ND-8).

CHAPTER V: CONCLUDING REMARKS

A system for the patterning of amines through the thermal decomposition of a thin polymer film was proposed. The polymer (**3**) was synthesized and its thermal and spectroscopic properties were explored. TGA demonstrated that the two different conformers present in the polymer possess different T_d , one beginning at 150 °C and accounting for 80 % of the carbamate moieties and the other beginning at 210 °C and accounting for the other 20 %. The pyrolysis of the polymer (**3**) was shown in solution to favor the decomposition pathway resulting in a primary amine relative to the isocyanate by a ratio of approximately 3 to 1. It would be beneficial if this ratio could be increased further and the elimination of the isocyanate as a possible pathway would be ideal. The adoption of alternate protecting groups would be the most logical first step in that direction.

Films of **3** were produced by spin coating and crosslinked through photo-processing. Spectroscopic analysis of the reactions that occur throughout the film during both processing and patterning was performed. The crosslinking of the cinnamate was observed by FT-IR and UV spectroscopy and the binding of the film to the substrate through a monolayer of benzophenone (**17**) was qualitatively demonstrated. The photo-processing of the polymer film was streamlined to a one-step process. The thermal reactions of the surface were analyzed by FT-IR spectroscopy and only the amine forming decomposition pathway was observed.

Post modification of these films was tested both in the bulk and on the μm scale. The heated material was either conjugated to a fluorescently labeled protein or to the

fluorescent dye FITC. Bulk characterization demonstrated a preference for the heated polymer film that had been treated with the homobifunctional crosslinker glutaraldehyde, as predicted. However, a heated sample without the glutaraldehyde crosslinker and an unheated sample treated with glutaraldehyde also demonstrated increased affinity for the protein. This affinity will reduce the possible contrast achievable by TCNL when using these surfaces and completely eliminate the possibility of single protein patterning until it can be prevented. TCNL was performed to create μm scale patterns of free amine. Both a fluorescently tagged Fibronectin molecule and FITC were bound to the pattern and fluorescent images were obtained. The resulting images indicated the protein did preferentially bind to the patterned areas, though the intensities were inconsistent, even within a single sample. This suggests there is a repeatability issue with TCNL when used with this system, even within single fabrication runs, that will need to be overcome. Despite issues regarding repeatability, the observed patterns did demonstrate that TCNL can be used with the designed polymer films of **3** to create distinctive patterns, though more refining of the technique is needed.

APPENDIX A

EXPERIMENTAL METHODS

Materials and Equipment:

Chemicals used for experiments were as follows: dodecylisocyanate (Acros), Dihydropyran (Aldrich), 2-isocyanatoethyl methacrylate (Aldrich), azobisisobutyronitrile (Aldrich), poly(p-xylene tetrahydrothiophenium chloride) (Aldrich), allyl bromide (Aldrich), chlorodimethyl silane (Alfa Aesar), 4-hydroxybenzophenone (Alfa Aesar), Bovine plasma fibronectin (EMD Bioscience), nitrobenzene-*d*₅ (ICN Biomedicals), platinum on activated carbon (10 % wt., Strem Chemicals), 1,8-diazabicyclo[5.4.0]undec-7-ene (TCI), potassium carbonate (VWR). All solvents were reagent grade. All chemicals were used as received with the exception of chlorodimethylsilane, which was distilled under nitrogen immediately before use.

Equipment used for analyses were as follows: Varian spectrophotometer (Cary 5E), Perkin Elmer FT-IR spectrometer (Spectrum 1000, reflectance measurements used a Perkin Elmer Fixed Angle Specular Reflectance accessory, angle of incidence = 16°), Rayonet photochemical reactor (RPR-100, 300 nm bulbs), Stratagene Stratalinker (model # 2400, 354 nm bulbs), Varian NMR spectrometer (Mercury Vx 300, 5 mm broadband probehead), VEECO atomic force microscope (Nanoscope Multimode IV) with Nanosensor cantilevers (SSS-NHCR), AST goniometer (VCA-2500XE), Veeco stylus profilometer (Deektak 6M), Laurell spin coater (WS-400B-6NPP-lite), and Nikon fluorescent microscope (TE2000 equipped with an Intensilight C-HGFIE light source, a Plan Apo 60x water immersion objective (Nikon, NA 1.2), DQC-FS EMCCD camera and

96320, FITC/GFP HyQ filter set, excitation 460-500 nm, dichroic mirror DM505, emission 510-560 nm).

Synthesis of tetrahydropyran-2-ol (5):

The synthesis of tetrahydropyran-2-ol was carried out according to a literature procedure.²⁹ The ¹H NMR spectrum was consistent with values reported in the literature.²⁹

Synthesis of tetrahydropyran-2-yl N-(2-methacryloxyethyl)carbamate (2):

Tetrahydropyran-2-ol (2.80 mL, 28 mmol) was mixed with 2-isocyanatoethyl methacrylate (3.1 g, 20 mmol) and 1 drop of pyridine and stirred until the reaction was complete by ¹H NMR. The resulting viscous mixture was purified by column chromatography on silica to yield a white powder (2.93 g, 57 %). ¹H NMR (300 MHz, CDCl₃): δ (ppm) 6.09 (m, 1H), 5.9 (broad, 0.2 H, minor conformer), 5.82 (broad, 0.8 H, major conformer), 5.57 (apparent quint, $J = 1.5$ Hz, 1H), 5.05 (broad, 0.8 H, major conformer *N-H*), 4.83 (broad, 0.2 H, minor conformer *N-H*), 4.21 (t, $J = 6$ Hz, 2H), 3.86 (ABXY m, $J_{AB} = 11.5$ Hz, $J_{AX} = 4.8$ Hz, $J_{AY} = 5.1$ Hz, 1H), 3.63 (ABXY m, $J_{AB} = 11.5$ Hz, $J_{AX} = 8.6$ Hz, $J_{AY} = 3.0$ Hz, 1H), 3.49 (q, $J = 6$ Hz, 2H), 1.91 (dd, $J = 1.5, 0.9$ Hz, 3H), 1.77 (apparent dd, $J = 9.7, 2.7$ Hz, 2H), 1.48-1.68 (m, 4H); ¹³C NMR (75 MHz, CDCl₃): δ (ppm) 167.2, 155.0, 135.9, 126.0, 93.3, 63.5, 63.3, 40.0, 29.3, 24.8, 19.0, 18.2. Anal. Calcd for C₁₂H₁₉NO₅: C: 56.02; H: 7.44; N: 5.44. Found: C: 56.22; H: 7.36; N: 5.48.

Synthesis of methyl 4-(3-methacryloyloxypropoxy)cinnamate (1):

The synthesis of methyl **1** was carried out according to a literature procedure.²⁸ ¹H NMR spectral features were consistent with reported values.²⁸

Synthesis of poly((tetrahydropyran-2-yl N-(2-methacryloxyethyl)carbamate)-co-(methyl 4-(3-methacryloyloxypropoxy)cinnamate)) (3):

A mixture of **2** (0.50 g, 1.9 mmol), **1** (0.15 g, 0.48 mmol), and azobisisobutyronitrile (AIBN) (2.0 mg, 0.012 mmol) in THF (6 mL) were added to a Schlenk ampoule using a Pasteur pipette. The flask was then freeze-pump-thawed a minimum of four times and the reaction mixture was heated at 60 °C for 20 h. Once the reaction mixture had returned to room temperature it was diluted with dichloromethane (30 mL) and added dropwise to hexanes (300 mL). The resulting precipitate was removed by vacuum filtration and dried under vacuum to yield a white powder (360 mg, 55 %). ¹H NMR (300 MHz, CDCl₃): δ (ppm) 7.6 (d broad, *J* = 16.1 Hz, 1H), 7.5 (s broad, 2H), 6.9 (s broad, 2H), 6.3 (d broad, *J* = 16.1 Hz, 1H), 5.7-6.0 (m broad, 5.2 H), 3.3-4.2 (four apparent singlets broad, 27.2 H), 0.7-2.1 (several m broad, 50.6 H); ¹³C NMR (75 MHz, CDCl₃): δ (ppm) 177.1, 167.8, 160.4, 155.3, 144.5, 129.8, 128.1, 127.8, 127.4, 127.2, 115.3, 114.8, 93.3, 63.6, 53.9, 51.6, 45.0, 44.7, 39.6, 39.5, 28.0, 25.0, 19.1, 17.4. Note: The ¹H-NMR spectrum is reported as observed, with integration relative to the peak at 7.5 ppm (2H, due to aromatic protons in the cinnamate group). The N-H protons were not observed in the spectrum of the polymer. Anal. Calcd for C₆₅H₉₆N₄O₂₅(1:4 cinnamate:carbamate monomer ratio): C: 58.55; H: 7.26; N: 4.20. Found: C: 57.83; H: 7.20; N: 4.12.

The results of the ^1H NMR spectrum would suggest a carbamate content slightly lower than the one expected for a cinnamate to carbamate feed ratio of 1 to 4, whereas the elemental analysis (based on carbon) would suggest a higher content of the carbamate component.

Synthesis of poly(tetrahydropyran-2-yl N-(2-methacryloxyethyl)carbamate) (10):

Polymerization was conducted in the same manner as for **3**. **2** (1.285 g, 5 mmol) and AIBN (16.4 mg, 0.1 mmol) were dissolved in THF (15 mL) and **10** was isolated as a white powder (1.09 g, 85 %). ^1H NMR (300 MHz, CDCl_3): δ (ppm) 6.7 (s broad, 1H), 6.2 (s broad, 1H), 6.9 (s broad, 2H), 3.6 – 4.7 (three apparent singlets broad, 6 H), 1.1 – 2.2 (four apparent singlets broad, 11 H).

Synthesis of tetrahydropyran-2-yl dodecylcarbamate (14):

To a solution of tetrahydropyran-2-ol (0.83 g, 8.1 mmol) in dichloromethane (30 mL) in an oven-dried Schlenk flask was added 1,8-diazabicyclo[5.4.0]undec-7-ene (DBU, 6.1 g, 40 mmol) followed by dodecylisocyanate (2.0 g, 9.5 mmol). The reaction was then stirred over the 48 hours before adding 100 mL saturated NH_4Cl and separating the two layers using a separatory funnel. The aqueous layer was then extracted using three 100 mL portions of DCM. The combined organic layers were washed with 200 mL of saturated NH_4Cl solution and 200 mL of saturated NaCl solution and then dried with MgSO_4 . The solvent was removed using a rotary evaporator and the solid was ran through a silica column eluting with 1 : 1 hexanes : ethylacetate to yield 1.98 g (80 %) of a light yellow powder. ^1H -NMR (CDCl_3 , 400 MHz): δ (ppm) 5.93 (broad, 0.13 H, minor

conformer), 5.82 (broad, 0.87 H, minor conformer), 4.75 (broad, 0.86H, major conformer), 4.52 (broad, 0.14H, minor conformer), 3.90 (ABXY, $J_{AB} = 11.5$ Hz, $J_{AX} = 8.4$ Hz, $J_{AY} = 3.1$ Hz, 1H), 3.67 (ABXY, $J_{AB} = 11.5$ Hz, $J_{AX} = 5.1$ Hz, $J_{AY} = 4.1$ Hz, 1H), 3.18 (q, $J = 6.2$ Hz, 2H), 1.79, (apparent dd, $J = 8.9$ Hz, 2.4 Hz, 2H), 1.62 (m, 4H), 1.50 (apparent quint., $J = 7.0$ Hz, 2H), 1.33-1.22 (m, 18 H), 0.87 (t, $J = 6.7$ Hz, 3H); ^{13}C -NMR (CDCl_3 , 100 MHz): δ (ppm) 155.98, 93.03, 63.45, 40.88, 31.84, 29.79, 29.57, 29.55, 29.51, 29.47, 29.46, 29.28, 29.21, 26.70, 24.92, 22.62, 19.20, 14.06. HRMS (FAB) Calcd for $\text{C}_{18}\text{H}_{36}\text{NO}_3$ (MH^+): 314.2695. Found 314.2667. Anal. Calcd for $\text{C}_{18}\text{H}_{35}\text{NO}_3$: C: 68.7; H: 11.25; N: 4.47. Found: C: 69.06; H: 11.46; N: 4.58.

Synthesis of 4-allyloxybenzophenone (16):³³

The synthesis of **16** was carried out according to a literature procedure.³³ ^1H NMR spectral features were consistent with reported values.³³

Synthesis of 4-(3-chlorodimethylsilyl)propoxy benzophenone (17):

The synthesis of **17** was carried out according to a literature procedure.³³ ^1H NMR spectral features were consistent with reported values.³³

Determination of the pyrolysis products of 10:

Approximately 50 mg of **10** was dissolved in 1.0 mL of nitrobenzene- d_5 and analyzed by ^1H NMR spectroscopy. The solution was refluxed for approximately one hour and then filtered through a pipette containing a piece of cotton before analyzing with ^1H NMR.

Determination of pyrolysis products of 14:

25 mg of **14** were dissolved with sonication in 0.50 mL of nitrobenzene-*d*₅ and transferred to a NMR tube. The NMR tube was placed in an oil bath preheated to 220 °C and allowed to reflux in the NMR tube for approximately 15 min. The tube was then removed from the oil bath and cooled to room temperature. The mixture in the NMR tube was analyzed by ¹H NMR at 80 °C and compared to a spectrum of **14** in nitrobenzene obtained at 80 °C.

Binding of 17 to glass substrates:

A procedure similar to the one reported in the literature was employed.³³ Specifically, glass slides or silicon wafers were cut into several 25 × 25 mm² squares then cleaned with either piranha (75 % concentrated H₂SO₄ and 25 % of 30 % H₂O₂ in water) or oxygen plasma. The slides or wafers were placed in anhydrous toluene (~50 mL) under argon and a solution of **17** in toluene (3 mL, ca. 0.28 M) was added along with enough anhydrous triethylamine that cloudiness of the liquid was observed (about 5 drops). The slides were left in the solution overnight and then washed with chloroform and dried under N₂. The presence of the benzophenone monolayer on the surface was confirmed by a contact angle measurement of 60 – 70°, consistent with reported values.³⁵

Polymer film preparation:

Enough drops of a solution of **3** in cyclohexanone (typical concentration of 20 mg / mL) were added to the surface of either glass slides or silicon wafers (25 × 25 mm²) that had

been treated with **17** as described above to completely wet the surface. The slides were then spun for 2 minutes at varying speeds (most commonly 1000 RPM). The slides were then either exposed to 352 nm radiation for one hour and 300 nm radiation for 45 minutes or they were exposed only to 300 nm radiation for 40 minutes. Films were prepared with thicknesses ranging from 30 – 150 nm, though most experiments were performed on films with a thickness of 75 ± 5 nm, as measured by stylus profilometry.

Spectral analysis of the effects of temperature on films of 3:

Several polymer films prepared on silicon wafers as above were analyzed by specular reflectance FTIR spectroscopy. The analysis chamber had been flushed with N₂ for a minimum of 10 minutes after changing each sample and a clean silicon wafer was used as a background. The slides were then exposed to UV irradiation (300 nm) for approximately 45 min and analyzed again. Each wafer was heated on a hot plate for 30 min. to one of the following temperatures 120, 150, 180, and 210 °C and again analyzed by FT-IR spectroscopy.

Spectral analysis of the effects of photo-treatment on films of 3:

Several films of polymer **3** were prepared on both silicon wafers and glass slides as above. Samples on silicon substrates were analyzed by specular reflectance FTIR spectroscopy. The analysis chamber was flushed with N₂ for a minimum of 10 minutes after changing each sample and a constant stream of N₂ was maintained during analysis. Samples on glass substrates were analyzed by UV spectroscopy. Half of the samples

were then exposed to UV irradiation (354 nm) for one hour. Spectra of each sample were obtained at regular intervals during irradiation with 300 nm radiation.

Bioconjugation to Fibronectin:

Several polymer samples were prepared as above and half were heated to 180 °C and half were left at room temperature. A 0.5 mg/ml solution of glutaraldehyde in deionized H₂O was prepared and added to the surface of one each of the heated and unheated films. Each slide was then washed with DI H₂O followed by phosphate buffer solution (PBS) solution, and exposed to a solution containing Atto-488 modified fibronectin. Images were obtained using a fluorescence microscope and the average intensity of fluorescence was measured.

Coating of poly(p-xylylene tetrahydrothiophenium chloride) onto glass slides.

Three 75 × 25 mm glass slides were scored into three 25 × 25 mm squares. They were cleaned by sonicating in ethanol for 10 minutes, drying with N₂ and then placing them in Piranha solution (75 % concentrated H₂SO₄ and 25 % H₂O₂) at 50 °C for at least 30 minutes. The slides were then snapped along the score marks. Two solutions of poly(p-xylylene tetrahydrothiophenium chloride) in water were prepared, one each of 12.5 % and 8.33 %. The slides were coated by adding 0.4 ml of one of the solutions and then spinning for two minutes at either 1000, 2000, or 3000 RPM. A UV lamp was used to determine the quality of the coating and a fluorescent microscope was used to image patterns that had been drawn in the polymer

REFERENCES

1. Kameyama, M.; McCallum, M., Extension of Photolithography. *Proceedings of SPIE* **2004**, 5446, 451 - 461.
2. Whitesides, G. M.; Ostuni, E.; Takayama, S.; Jiang, X.; Ingber, D. E., Soft Lithography in Biology and Biochemistry. *Annu. Rev. Biomed. Eng* **2001**, 3, 335 - 373.
3. Tseng, A. A.; Notargiacomo, A.; Chen, T. P., Nanofabrication by scanning probe microscope lithography: A review. *J. Vac. Sci. Technol. B* **2005**, 23, 877 - 894.
4. Binnig, G.; Rohrer, H.; Gerber, C.; Weibel, E., Surface Studies by Scanning Tunneling Microscopy. *Phys. Rev. Lett.* **1982**, 49, 57 - 61.
5. Tinazli, A.; Piehler, J.; Beuttler, M.; Guckenberger, R.; Tampe, R., Native protein nanolithography that can write, read and erase. *Nat. Nanotechnol.* **2007**, 2, 220 - 225.
6. Piner, R. D.; Zhu, J.; Xu, F.; Hong, S.; Mirkin, C. A., "Dip-Pen" Nanolithography. *Science* **1999**, 283, 661 - 663.
7. Salaita, K.; Wang, Y.; Mirkin, C. A., Applications of Dip-Pen Nanolithography. *Nat. Nanotechnol.* **2007**, 2, 145 - 155.
8. Jang, J.-W.; Maspoeh, D.; Fujigaya, T.; Mirkin, C. A., A "Molecular Eraser" for Dip-Pen Nanolithography. *Small* **2007**, 3, 600 - 605.
9. Szoszkiewicz, R.; Okada, T.; Jones, S. C.; Li, T.-D.; King, W. P.; Marder, S. R.; Riedo, E., High-Speed, Sub-15 nm Feature Size Thermochemical Nanolithography *Nano Lett.* **2007**, 7, 1064 - 1069.
10. Vettiger, P.; Despont, M.; Drechsler, U.; Durig, U.; Haberle, W.; Lutwyche, M. I.; Rothuizen, H. E.; Stutz, R.; Widmer, R.; Binnig, G. K., The "Millipede" — More than One Thousand Tips for Future AFM Data Storage. *IBM J. Res. Develop.* **2000**, 44, 323 - 340.
11. Gotsmann, B.; Duerig, U.; Frommer, J.; Hawker, C. J., Exploiting Chemical Switching in a Diels–Alder Polymer for Nanoscale Probe Lithography and Data Storage. *Adv. Funct. Mater.* **2006**, 16, 1499–1505.
12. Durig, U.; Crossa, G.; Despont, M.; Drechsler, U.; Haberle, W.; Lutwychea, M. I.; Rothuizen, H.; Stutza, R.; Widmer, R.; Vettiger, P.; Binnig, G. K.; King, W. P.; Goodson, K. E., "Millipede" – an AFM data storage system at the frontier of nanotribology. *Tribology Letters* **2000**, 9, 25–32.

13. Wang, D. B.; Szoszkiewicz, R.; Lucas, M.; Riedo, E.; Okada, T.; Jones, S. C.; Marder, S. R.; Lee, J.; King, W. P., Local wettability modification by thermochemical nanolithography with write-read-overwrite capability. *Appl. Phys. Lett.* **2007**, 91, 243104-1 - 243104-3.
14. Zou, S.; MasPOCH, D.; Wang, Y.; Mirkin, C. A.; Schatz, G. C., Rings of Single-Walled Carbon Nanotubes: Molecular-Template Directed Assembly and Monte Carlo Modeling. *Nano Lett.* **2007**, 7, 276 - 280.
15. Basu, A. S.; McNamara, S.; Gianchandani, Y. B. J., Scanning thermal lithography: Maskless, Submicron Thermochemical Patterning of Photoresist by Ultracompliant Probes. *J. Vac. Sci. Technol. B* **2004**, 22, 3217 - 3220.
16. Gallucci, R. R., Preparation and Reactions of Carbamate-Modified Polyethylene. *J. Appl. Polym. Sci.* **1981**, 26, 249 - 260
17. Al-Awadi, N.; Bigley, D. B., Carbonate Pyrolysis. Part 6.1 The Kinetics and Mechanism of the Pyrolysis of Thion- and Dithio-carbonates. Implications for the Transition State in Carbonate Pyrolysis. *J. Chem. Soc. Perkin Trans. II* **1982**, 773 - 775.
18. Bigley, D.; Wren, C. M., Pyrolysis of carbonates. Part I. The gas-phase pyrolysis of some symmetrical primary alkyl carbonates. *J. Chem. Soc. Perkin Trans. II* **1971**, 926 - 928.
19. Hermanson, G. T., *Bioconjugate Techniques*. Oxford, Academic Press.: 1996.
20. Mrksich, M., A Surface Chemistry Approach to Studying Cell Adhesion. *Chem. Soc. Rev* **2000**, 29, 267 - 273.
21. Mrksich, M.; Dike, L. E.; Tien, J.; Ingber, D. E.; Whitesides, G. M., Using Microcontact Printing to Pattern the Attachment of Mammalian Cells to Self-Assembled Monolayers of Alkanethiolates on Transparent Films of Gold and Silver. *Exp. Cell. Res.* **1997**, 235, 305 - 313.
22. Hoover, D. K.; Chan, E. W. L.; Yousaf, M. N., Asymmetric Peptide Nanoarray Surfaces for Studies of Single Cell Polarization. *J. Am. Chem. Soc.* **2008**, 130, 3280 - 3281.
23. Yu, A. A.; Savas, T. A.; Taylor, G. S.; Guiseppe-Elie, A.; Smith, H. I.; Stellacci, F., Supramolecular Nanostamping: Using DNA as Movable Type. *Nano Lett.* **2005**, 5, (6), 1061 - 1064.
24. Jayakrishnan, A.; Jameela, S. R., Glutaraldehyde as a Fixative in Bioprotheses and Drug Delivery Matrices. *Biomaterials* **1996**, 33, 471 - 484.
25. Backer, S. A.; Suez, I.; Fresco, Z. M.; Rolandi, M.; Fréchet, J. M. J., Covalent Formation of Nanoscale Fullerene and Dendrimer Patterns. *Langmuir* **2007**, 23, (5), 2297 - 2299.

26. Dyer, E.; Osborne, W., The Thermal Degradation of a Polythiolcarbamate. *J. Polym. Sci.* **1960**, 47, 349 - 350.
27. Dyer, E.; Read, R. E., Thermal Degradation of 0-1-Hexadecyl N-1-Naphthylcarbamates and Related Compounds. *J. Org. Chem.* **1961**, 26, 4388 - 4394.
28. Zhang, Y.-D.; Hreha, R. D.; Jabbour, G. E.; Kippelen, B.; Peyghambarian, N.; Marder, S. R., Photo-crosslinkable polymers as hole-transport materials for organic light-emitting diodes. *J. Mater. Chem.* **2002**, 12, 1703 - 1708.
29. Kimura, M.; Shimizu, M.; Tanaka, S.; Tamaru, Y., *Tetrahedron* **2005**, 61, 3709 - 3718.
30. Booth, H.; Khedhair, K. A.; Readshaw, S., Experimental Studies of the Anomeric Effect Part I: 2-Substituted Tetrahydropyrans. *Tetrahedron* **1987**, 43, (20), 4699 - 4723.
31. Osakai, T.; Hoshino, M.; Izumi, M.; Kawakami, M.; Akasaka, K., Proton NMR Study on Selective Hydration of Anions in Nitrobenzene. *J. Phys. Chem. B* **2000**, 104, 12021 - 12027.
32. Hornback, J. M., *Organic Chemistry*. Brooks/Cole Publishing Company: 1998.
33. Prucker, O.; Naumann, C. A.; Ruhe, J.; Knoll, W.; Frank, C. W., Photochemical Attachment of Polymer Films to Solid Surfaces via Monolayers of Benzophenone Derivatives. *J. Am. Chem. Soc.* **1999**, 121, 8766 - 8770.
34. Dormtin, G.; Prestwich, G. D., Benzophenone Photophores in Biochemistry. *Biochemistry* **1994**, 33, 5661 - 5673.
35. Griep-Raming, N.; Karger, M.; Menzel, H., *Langmuir* **2004**, 20, 11811 - 11814.
36. Hester, R. E.; Clark, R. J. H., *Spectroscopy for Surface Science*. John Wiley & Sons: Chichester, 1998; Vol. 26, p 399.
37. Silverstein, R. M.; Webster, F. X.; Kiemle, D. J., *Spectrometric Identification of Organic Compounds*. 7 ed.; John Wiley & Sons, Inc.: 2005; p 502.
38. Turek, A. M.; Krishnamoorthy, G.; Phipps, K.; Saltiel, J., Resolution of Benzophenone Delayed Fluorescence and Phosphorescence with Compensation for Thermal Broadening. *J. Phys. Chem. A* **2002**, 106, (25), 6044 - 6052.
39. Robeson, J. L.; Tilton, R. D., Potassium-Dependent Slow Inactivation of Kir1.1 (ROMK) Channels *Biophys. J.* **1995**, 68, 2145 - 2155.
40. Bradley, D. D. C., Precursor-Route poly(p-phenylenevinylene): Polymer Characterisation and Control of Electronic Properties. *J. Phys. D: Appl. Phys* **1987**, 20, (11), 1389 - 1410.

41. Henckens, A.; Duyssens, I.; L., L.; Vanderzande, D.; Cleij, T. J., Synthesis of Poly(p-phenylene vinylene) and Derivatives via a new Precursor Route, the Dithiocarbamate Route. *Polymer* **2005**, 47, 123 - 131.
42. Antoun, S.; Gagnon, D. R.; Karasz, F. E.; Lenz, R. W., Preparation and electrical conductivity of poly(1,4-naphthalene vinylene). *J. Polym. Sci, Part C: Polym Lett.* **1986**, 24, (10), 503 - 509.
43. Stenger-Smith, J. D.; Lenz, R. W.; Wegner, G., Spectroscopic and cyclic voltammetric studies of poly(p-phenylene vinylene) prepared from two different sulphonium salt precursor polymers. *Polymer* **1989**, 30, (6), 1048 - 1053.